The Application of Isotropic Bicelles as Model Membranes

Doctoral Thesis in Biophysics

August Andersson

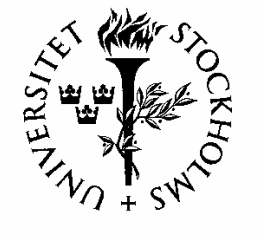

Department of Biochemistry
and Biophysics
Stockholm University
Spring 2005

Cover illustration:
An α-helix structure is induced in the peptide hormone motilin upon binding to a bicelle

Doctoral thesis in Biophysics

ISBN 91-7155-043-7
Printed by Akademitryck AB, Valdemarsvik 2005

Abstract

Isotropic bicelles are disc-shaped aggregates of lipids and detergents, and are suitable model systems for high-resolution NMR studies of membrane-interacting peptides. In this thesis the structures for the two peptides motilin and transportan were determined by homonuclear ^{1}H methods in the presence of bicelles, and the structure of the bovine prion protein peptide (bPrPp) was solved in the presence of DHPC micelles. All of these peptides were found to be largely α-helical when bound to the model membranes. In subsequent experiments both motilin and transportan were shown to reside on the surface of the bicelles, whereas bPrPp is more likely to have a transmembrane configuration.

NMR translational diffusion experiments revealed that the isotropic bicelles studied here are very large objects compared to what is regularly indicated by high-resolution NMR spectroscopy. Furthermore, these studies showed that all three peptides examined interact strongly with bicelles. Investigation of the NMR-relaxation of labeled sites in the peptides motilin and penetratin demonstrated that the overall rotational correlation times for these peptides do not reflect the bicellar size. Such decoupling of NMR relaxation from the dependence of overall size is also seen for the dynamics of the lipid molecules in the bicelles. It is therefore concluded that the overall size is not the sole determinant of the linewidths in NMR spectra, but that extensive motions within the bicelles also exert significant effects.

Another interesting observation is that the membrane-bound structures of the peptides motilin, transportan, penetratin and bPrPp are very similar, even though these peptides have very different biological functions. In contrast, considerably more variation is observed in the membrane-positioning and molecular dynamics of these peptides. Since the bicelles have been found to induce differences in membrane positioning and molecular dynamics compared to micelles, these model membranes are likely to be important in order to enhance our understanding of the biological function of membrane interacting peptides.

Table of Contents:

List of publications

This thesis is based on the following articles, which will be referred to in the text by their Roman numerals:

I. Andersson, A., and L. Mäler. 2002. NMR solution structure and dynamics of motilin in isotropic phospholipid bicellar solution. *J. Biomol. NMR* 24:103-112

II. Andersson, A., and L. Mäler. 2003. Motilin-bicelle interactions: membrane position and translational diffusion. *FEBS Lett.* 545:139-143

III. Andersson, A., J. Almqvist, F. Hagn and L. Mäler. 2004. Diffusion and dynamics of penetratin in different membrane mimicking media. *Biochim. Biophys. Acta* 1661:18-26

IV. Bárány-Wallje, E., A. Andersson, A. Gräslund and L. Mäler. 2004. NMR solution structure and position of transportan in neutral bicelles. *FEBS Lett.* 567:265-269

V. Biverståhl, H., A. Andersson, A. Gräslund and L. Mäler. 2004. NMR solution structure and membrane interaction of the N-terminal sequence (1-30) of the bovine prion protein. *Biochemistry* 43:14940-14947

VI. Andersson, A., and L. Mäler. 2005. Magnetic resonance investigations of lipid motion in isotropic bicelles. *Submitted for publication*

Abbreviations:

aa	amino acid
AFM	atomic force microscopy
bPrPp	bovine prion protein peptide (1 - 30)
BWR	Bloch-Wangsness-Redfield
CD	circular dichroism
CMC	critical micelle concentration
CHAPS	3-[(3-cholamidopropyl)dimethylammonio]-1-propanesulfonate
CHAPSO	3-[(3-cholamidopropyl)dimethylammonio]-2-hydroxyl-1-propanesulfonate
COSY	correlation spectroscopy
CPP	cell-penetrating peptide
CSA	chemical shift anisotropy
DHPC	L-α-1,2-dihexanoylphosphatidylcholine
DLPC	1,2-dilauroyl-*sn*-glycero-3-phosphocholine
DLS	dynamic light scattering
DMPC	1,2-dimyristoyl-*sn*-glycero-3-phosphocholine
DMPG	1,2-dimyristoyl-*sn*-glycero-3-phospho-1-glycerol
DOXYL	2-(3-carboxylpropyl)-4,4dimethyl-2-tridecyl-3-oxazolidinyloxy
DPH	diphenylhexatriene
DPPC	1,2-palmitoyl-*sn*-glycero-3-phosphocholine
EM	electron microscopy
EPR	electron paramagnetic resonance
ESR	electron spin resonance
FAD	fluoresence anisotropy decay
FCS	fluoresence correlation spectroscopy
FID	free induced decay
F_p	Perrin shape factor
FRET	Förster radius energy transfer
FT	Fourier transform
GPCR	G-protein-coupled receptor
HFP	hexafluoropropanol
HSQC	heteronuclear single quantum coherence
L_α	lamellar liquid crystalline phase
L_β	lamellar gel phase
LUV	large unilamellar vesicle
MAS	magic-angle spinning
NLS	nuclear localization sequence
NMR	nuclear magnetic resonance
NOESY	nuclear Overhauser effect
PFG	pulsed field gradient
POPC	1-palmitoyl-2-oleoyl-*sn*-glycero-3-phosphocholine
R_1	longitudinal relaxation rate (inverse of T_1)
R_2	transverse relaxation rate (inverse of T_2)
RMSD	root mean squared deviation
S	order parameter
SDS	sodium dodecyl sulfate
ssNOE	steady state NOE
SUV	small unilamellar vesicle

T_1	longitudinal relaxation time
T_2	transverse relaxation time
TEMPO	2,2,6,6,-tetramethylpiperidinooxy
TMS	tetramethylsilane
TOCSY	total correlation spectroscopy
TROSY	transverse relaxation optimized spectroscopy
TSPA	3-methylsilyl-propionic acid

'In addition, biology as a whole would benefit from the physicist's general modus operandi, i.e., from the well-honed understanding of what science is and how it should be done: the crisp framing of problems, the clear understanding of what is and what isn't established truth, the importance of hypothesis testing, and the physicist's disinterested approach in general.'

Carl Woese
(Woese, 2004)

Ensam med en geting i vedboden
anade jag något

Tomas Tidholm

INTRODUCTION

The biological membrane, one of the key structural elements in all types of living cells, is involved in a multitude of important functions, including photosynthesis, respiration and signaling with the immediate environment. Biomembranes are not only required by all living organisms, but are also thought to have played a major role in prebiotic evolution and the origin of life (Deamer, 1997). Many interesting features of biomembranes have been explored employing several experimental and theoretical approaches.

The present thesis focuses on experimental characterization of the interaction of peptides with model membranes. For this purpose artificial mixtures of lipids and/or detergents are utilized to mimic the key physical properties of actual biomembranes. The choice of a specific type of model membrane depends both on the biomembrane which is being mimicked and on the experimental procedures to be applied.

Since the primary experimental method employed in the present study was solution-state nuclear magnetic resonance (NMR), it was important that the model membrane used reorients sufficiently rapidly to obtain good spectral resolution. This requirement imposes a rather strong restriction on the types of model membranes that are suitable. Micelles, which have classically been the major model membrane for solution-state NMR studies suffer from at least two major disadvantages, i.e., they are composed of detergents, rather than the natural lipid components of membranes, and they exhibit a strong curvature.

During the last ten years, bicelles have been introduced as a model membrane potentially superior to micelles (Marcotte and Auger, 2005). These mixtures of detergents and lipids are thought to form disc-shaped aggregates, with a central lipid bilayer and a detergent circumference (Figure 1). The presence of natural lipids and the fact that the surface of the central lipid region is more-or-less flat eliminate some of the limitations associated with micelles.

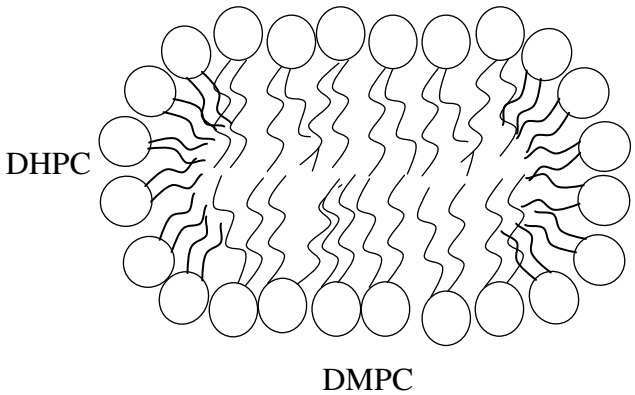

Figure 1 Schematic cross-section of a DMPC/DHPC bicelle, depicting DHPC molecules capping the ends of the central DMPC-rich region.

The work presented here was designed to characterize the interaction of bicelles with several different peptides with two principal concerns: in part, to understand how these peptides interact with a biological membrane, but also to elucidate the membrane-like properties of the bicelles. Our findings have also been

compared with those on other systems, e.g., by comparing the membrane-like properties of micelles and different types of bicelles.

It is highly interesting that both of these systems can be investigated using solution-state NMR methods. More challenging is the comparison of bicelles with other model systems such as vesicles, which are too large for this methodology. In such cases spectroscopic methods that can be applied to both types of model membranes, and are independent of rapid reorientation, not only allow valuable comparisons, but also complement and confirm the results obtained with NMR. Accordingly, spectroscopic approaches such as circular dichroism (CD) and electron paramagnetic resonance (EPR) have also been applied here.

The present investigation of peptide-bicelle interactions focuses on four different peptides, i.e., the gastrointestinal hormone motilin, the two cell-penetrating peptides (CPP) penetratin and transportan, and the N-terminal region (1-30) of the bovine prion protein (bPrPp). All these peptides, which have previously been characterized in other model systems, are thought to interact with membranes in rather different fashions. Here, we demonstrate that the interaction of these peptides with membranes can be studied effectively using bicelles as a membrane mimetic.

These interactions are similar in a number of ways, e.g, all the peptides exhibit strong binding to the bicelles accompanied by induction of an α-helix. However, differences were also observed. Motilin, transportan and penetratin are all prone to be localized at the surface of the membrane, whereas bPrPp tends to assume a transmembrane configuration. Moreover differences in local dynamics were apparent, e.g., the motion of motilin changes radically when 30% of the bicellar lipids contain negatively charged headgroups. Such differences can be correlated with the physical properties of the membranes to which these peptides are native and may influence the physiological activity of the peptide.

In addition to such studies on peptide interactions with bicelles, the lipids themselves in the bicelles were examined. One particular major problem associated with isotropic bicellar solutions is that the apparent size of the typical aggregate appears to be far too large for high-resolution NMR spectroscopy. However, this turns out not to be the case and it has been speculated that the spectral resolution in this situation is governed by extensive internal motion within the bicelle. Here, this hypothesis was tested and found to provide a reliable explanation of the data observed. However, a rather delicate balance between the overall size of the bicelles and the extent of local motion is expected, as demonstrated by, e.g., the peptide transportan, for which increasing the bicelle size by a factor of 1.5 renders the NMR spectra too broad to allow assignment.

This thesis consists of three parts. In the first part, (chapters 2 - 4) the background for the experimental studies performed is provided. Thus, chapter 2 is an introduction to biological membranes and peptides, the Brownian motion of molecules is discussed in chapter 3, and finally, chapter 4 describes our experimental approach, and the information that can be attained. The second part, consisting of chapter 5, summarizes and discusses the experimental findings, making comparisons between the different studies and to investigations reported in the literature. Finally, the research articles on which this thesis is based are appended.

Part 1: Background

2. BIOLOGICAL BACKGROUND

2.1 Biological membranes

The typical biological membrane is a complex structure composed primarily of lipids and proteins. Such membranes surround every living cell and also divide the interior of cells into compartments, such as organelles in eukaryotes. Different membranes contain sometimes very different types and relative amounts of lipids and proteins and this composition is influenced by the physiological status, changing in response to various stimuli. The basic structure of biological membranes consists of an amphipathic lipid layer, with a hydrophilic exterior and hydrophobic core (Figure 2).

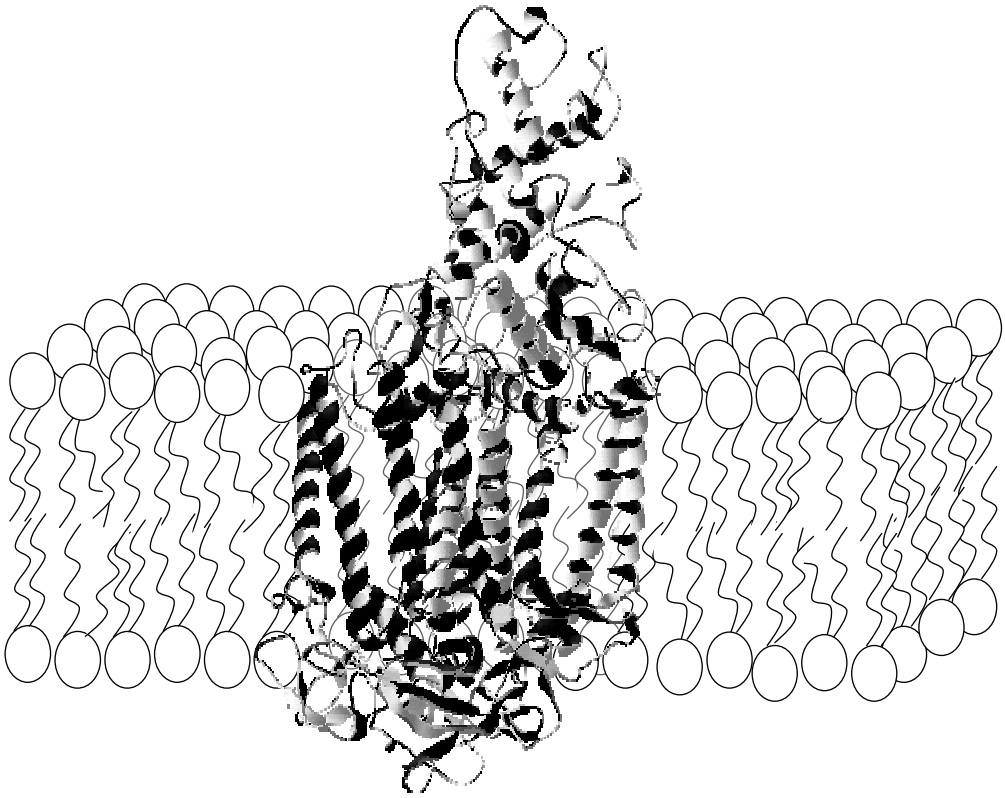

Figure 2 Schematic representation of a biological membrane bilayer with lipids () and a transmembrane membrane protein, in this case the photosynthetic reaction center from the purplebacterium *Rhodopseudomonas viridis* (Deisenhofer and Michel, 1989).

In most cells this structure is a bilayer, but in some organisms (typically archea) monolayers are present instead.

The major structural component of the bilayer is lipids of various kinds. In eukaryotes the most common type of lipids are phosphatidylcholines, whereas in prokaryotes (such as *Escherichia coli*), the main lipids are typically phosphatidylethanolamines (Gennis, 1989). One example of a typical eukaryotic

neutral (zwitterionic) phospholipid is POPC. The molecular structure of POPC is compared to those of DMPC and the negatively charged DMPG in Figure 3.

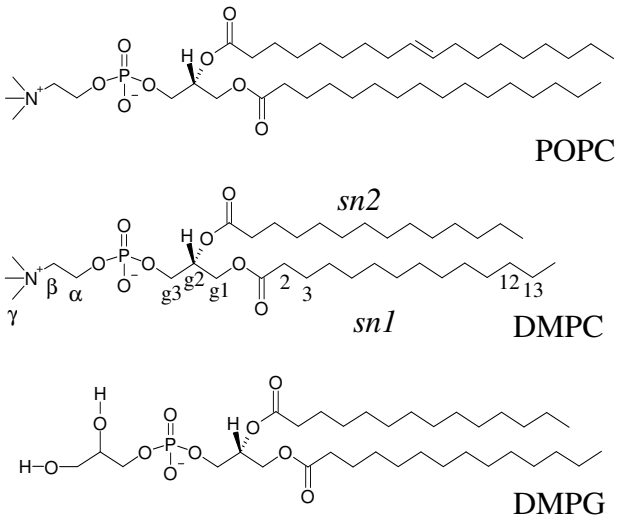

Figure 3 The molecular structures of POPC, DMPC and DMPG. The nomenclature for the positioning of the two fatty acyl chains is indicated for DMPC, as is the conventional numbering and labeling of some of the carbon atoms.

The paradigm concerning the structure and dynamics of biological membranes has long been the fluid-mosaic model (Singer and Nicolson, 1972), which postulates that the membrane is not a static two-dimensional crystal, but rather a highly dynamic system, with many types of motion. The term 'fluid-mosaic' indicates that the molecules within the membrane have considerable lateral and rotational freedom and are therefore randomly distributed within the membrane. Recently, however, structured subdomains of membranes have been identified (Vereb et al., 2003).

Even though such domains might be of considerable importance, biological membranes in general are highly dynamic, involving many modes of motion. These movements include rotations and translations of individual lipid molecules, collective motions of several lipid molecules together, as well as local movements of parts of a lipid molecule. These all occur on very different time-scales, as indicated by their correlation times (Figure 4). Both the amplitude and the frequency of these motions differ significantly in different membranes and are influenced by features such as curvature-induced stress and the packing of different types of lipids. These differences are finely tuned by the cell in order to control properties such as membrane permeability and resistance to mechanical stress.

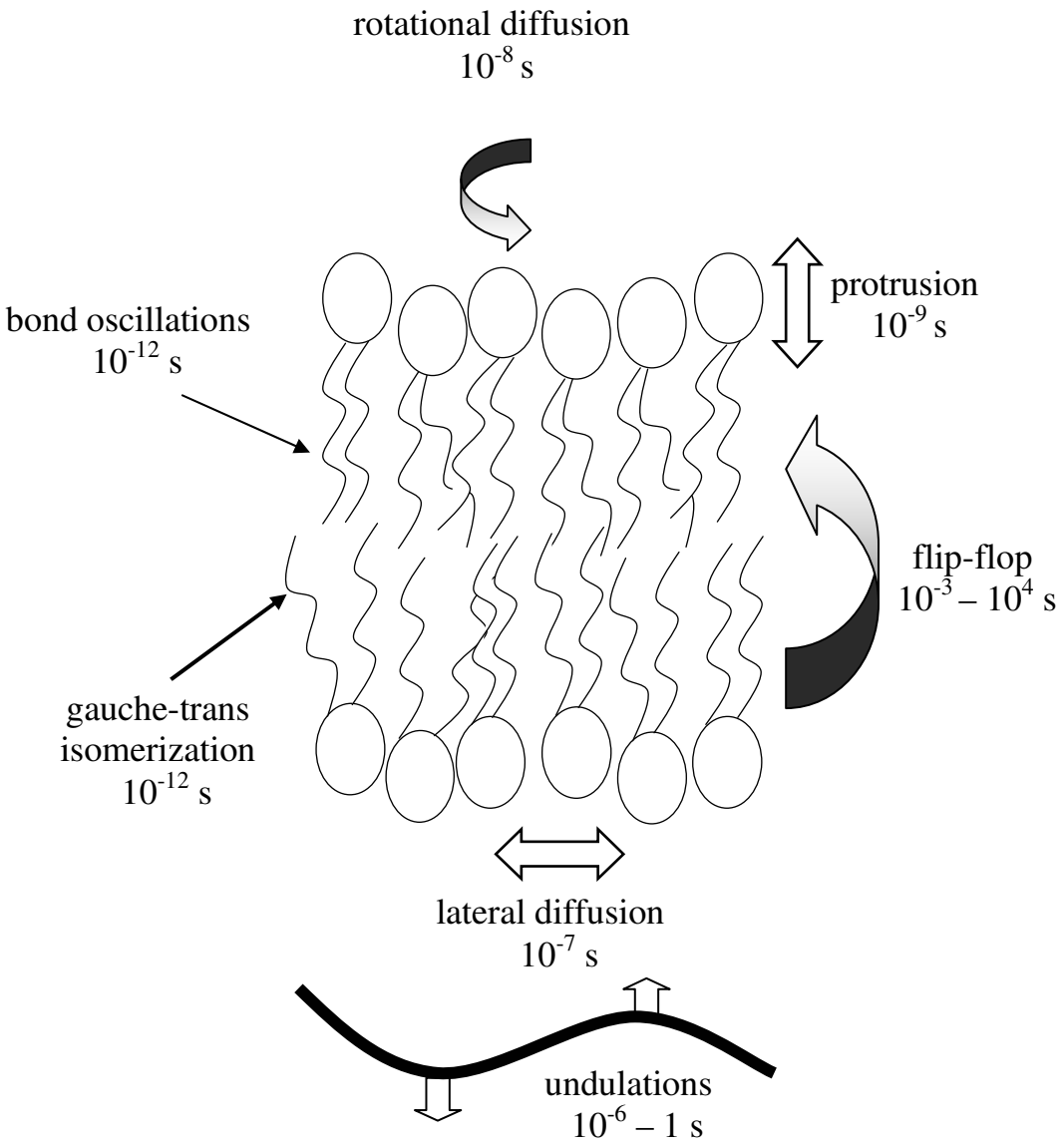

Figure 4 Typical time-scales (correlation times) for different types of motions in a biological membrane (adapted from (Yeagle, 2005)).

A general unifying theme for living cells is that their biological membranes, more-or-less, exist in the same phase, the lamellar liquid crystalline phase (L_α), which also is known as the fluid phase. However, this is but one out of the many possible phases that lipid mixtures can adopt. For instance, the fluid phase is very different from the gel phase (L_β), another lamellar phase, characterized by a higher degree of order. Transition from the fluid to the gel phase is commonly induced by lowering the temperature below a certain transition point. In order for studies with model membranes to be biologically relevant it is important that the fluid phase is predominant. Typical values for the various properties of fluid-phase vesicles containing DMPC are documented in Table 1.

Table 1 Typical physical properties of DMPC-containing vesicles in the fluid phase.

Property	Value	Reference
Membrane thickness[a]	44.2 Å	(Nagle and Tristram-Nagle, 2000)
Thickness of the fatty acyl core	26.2 Å	(Nagle and Tristram-Nagle, 2000)
Volume of a molecule of DMPC	1100 $Å^3$	(Nagle and Tristram-Nagle, 2000)
Rate of lateral diffusion	$10^{-11} m^2/s$	(Orädd and Lindblom, 2004)
Gel phase / fluid phase transition temperature ($L_\beta \rightarrow L_\alpha$)	298 K	(Hinz and Sturtevant, 1972)
Water permeability	6 μm/s	(Carruthers and Melchior, 1983)
Flip/flop half-time	9h	(Wimley and Thompson, 1990)
$D_\perp$[b]	$3.3*10^7\ s^{-1}$	(Mayer et al., 1990)
$D_\parallel$[b]	$3.3*10^8\ s^{-1}$	(Mayer et al., 1990)
S_{lipid}[c]	0.58	(Ellena et al., 1993)

a Steric thickness, without hydration

b $D_\parallel$ and $D_\perp$ are the overall rotational diffusion coefficients, around and perpendicular to the main axis, respectively

c S_{lipid} is the order parameter for the overall lipid motion.

The lipid molecules in a biological membrane are very dynamic in many respects, but on the average they are ordered locally along the transverse plane of the bilayer. In terms of liquid crystals, the membrane normal forms a local director for the lipids. Indeed, on a local scale the membrane is a lyotropic liquid crystal, a fact that is not only of fundamental significance, but also has consequences for spectroscopic studies.

Lipid membranes demonstrate low permeability to charged and polar molecules and, furthermore, exhibit the properties of an electrical insulator, like a capacitor, when an external electrical field is applied across them. As a consequence it is possible to create chemical (osmotic) and electrical gradients across membranes. In living cells such gradients are of central importance in processes such as photosynthesis, respiration and neural signal transmission.

For many cells, the outer membrane is the only structural line of defense (as well as spatial definition) in respect to the external world. The difficulties involved in the passage of polar or charged molecules across the membrane impose fundamental restrictions on how peptides and proteins interact with membranes. Processes such as the insertion of membrane proteins must be highly orchestrated and the detailed mechanisms of the transmembrane translocation of many molecules, including peptides remain to be elucidated.

2.2 Model membrane systems

The term model membrane is somewhat operational, being related to the aspects of a biological membrane that are being studied. In some cases a mixture of water and an organic solvent, such as the fluoro-alcohols TFE or HFP, is adequate to mimic a membrane mimetic environment. In general, however, such mixtures are

poor model systems, since the amphiphilic nature of biological membranes is not present.

In addition, the experimental technique being employed to examine a model membrane limits the number of possible mimetics. For instance, certain techniques require a solid-state type of membrane mimetic, such as bilayers stacked on glass surfaces, or monolayers of lipids deposited on a surface. Here, only dispersed membrane systems will be considered.

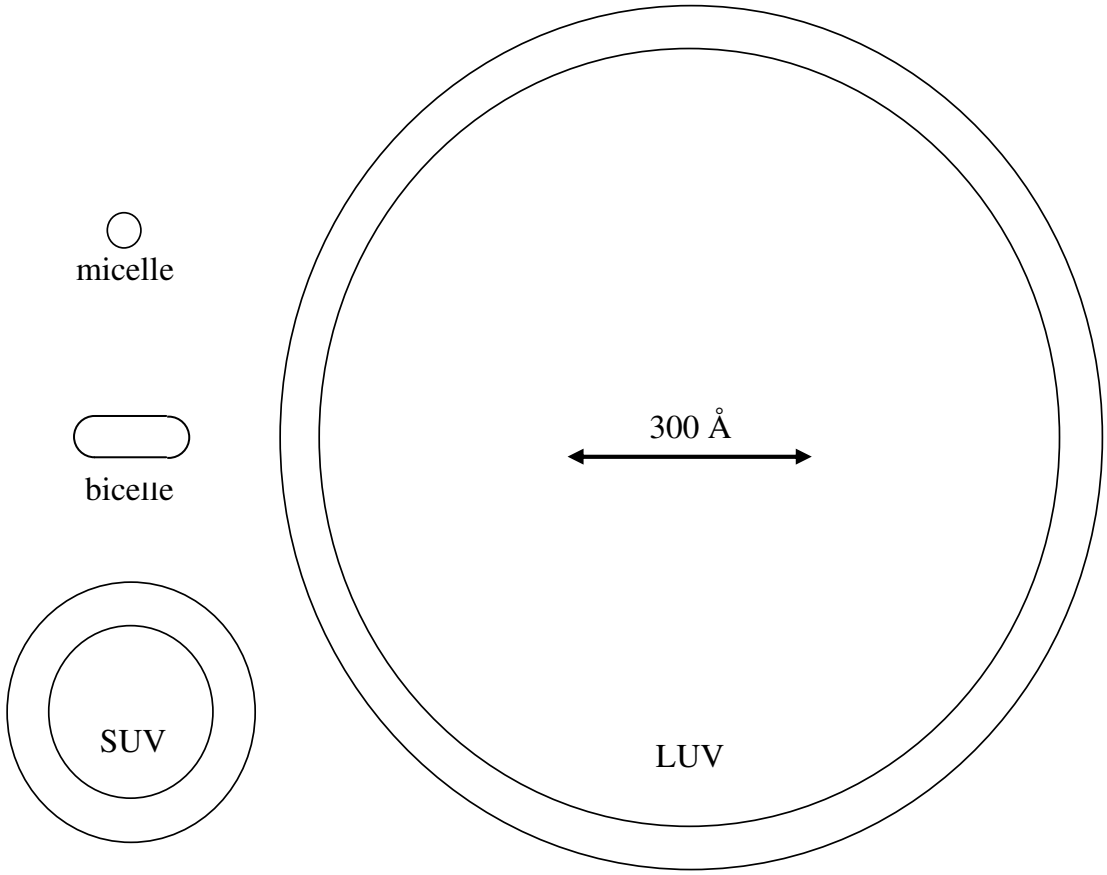

Figure 5 Relative sizes and shapes of a typical micelle, a bicelle (q = 0.5), a small unilamellar vesicle (SUV) and a large unilamellar vesicle (LUV) (Vold and Prosser, 1996; Pencer et al., 2001).

The membrane model that, from many perspectives, is most similar to natural biomembranes involves vesicles, sometimes also referred to as liposomes (Figure 5). The vesicles are water-filled spheres delineated by lipid bilayers. The typical biologically relevant vesicle is unilamellar, meaning that only a single bilayer structure is present in each vesicle. Due in part to the relatively large size of such vesicles, but also to the low concentrations of lipids that can be used to form stable vesicle dispersions, such model membranes are not suitable for most NMR investigations (Henry and Sykes, 1994).

For NMR studies, the micellar membrane model is preferred for a number of reasons. Micelles are relatively small (Table 2, Figure 5) which means that they rotate rapidly, on the time-scale required for NMR. Theses micelles consist of detergent molecules that aggregate above a certain threshold concentration called the critical micelle concentration (CMC). The size of a micelle is defined by the aggregation number, i.e., the average number of detergent molecules present. An increase in the

detergent concentration above the CMC results in the formation of more micelles, rather than larger micelles. Examples of detergents that form micelles are DHPC, SDS and CHAPS, the chemical structures of which are depicted in Figure 6, and some of the characteristic physical properties of the micelles formed by these detergents are presented in Table 2.

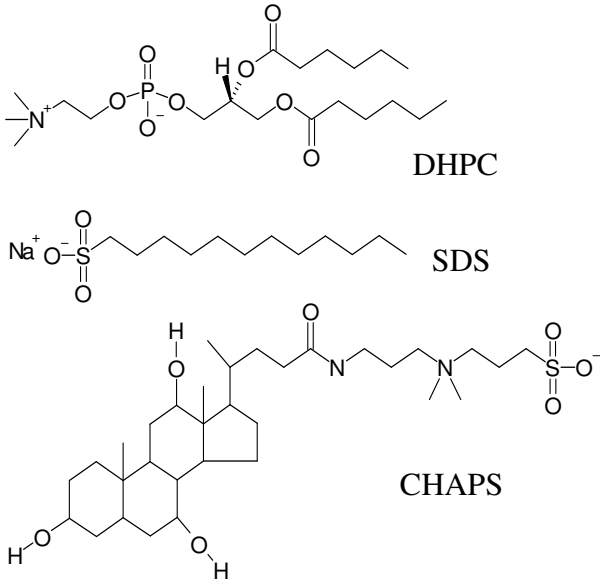

Figure 6 Molecular structures of the detergents DHPC, SDS and CHAPS

Table 2 Typical properties of the micelles formed by DHPC, SDS and CHAPS at temperatures near to 37 ^{o}C

	DHPC	**SDS**	**CHAPS**
Aggregation number	27[a]	64[b]	8[c]
Radius	18Å·18Å·30Å[d]	17 Å[e]	Not known
CMC	14 mM[f]	8 mM[b]	6 mM[g]

a (Chou et al., 2004)
b (Anlansson et al., 1976)
c (Funasaki et al., 1991)
d DHPC micelles have been shown to have a prolate shape (Lin et al., 1986)
e (Itri and Amaral, 1991)
f (Hauser, 2000)
g (Chattopadhyay and Harikumar, 1996)

The two major drawbacks of micelles as membrane-mimicking models are that they are composed of detergents and exhibit a strong curvature. A recent improvement in this connection was the discovery of bicelles, i.e., disc-shaped aggregates formed by mixing certain lipids and detergents at specific ratios (Figure 1).

The properties of such bicelles are dependent on several physical parameters, but one key feature is the *q*-value, which is defined as the molar ratio between lipid and detergent:

$$q = \frac{[\text{lipids}]}{[\text{detergents}]} \qquad (1)$$

Larger values of *q* give rise to aggregates with a more pronounced disc-like shape. At low *q*-values, bicelles are isotropically tumbling objects. However, above the phase transition temperature of DMPC and above a certain threshold *q*-value, a lyotropic liquid crystal is formed in the presence of strong magnetic fields. This reflects the fact that since the anisotropic molecular magnetic susceptibility of the lipid molecules exhibits a preferred orientation in a magnetic field and when this field is stronger than the force of free tumbling, sample alignment occurs (Hare et al., 1995).

The phase behavior of bicelles with large *q*-values has been found to be highly multifaceted and conflicting theories have been presented as to whether a bicellar solution consists of discs, or whether a completely different phase is formed (Gaemers and Bax, 2001; Arnold et al., 2002; Nieh et al., 2004; van Dam et al., 2004; Triba et al., 2005). In the present discussion, we will focus on the isotropic phase formed by bicelles with $q \leq 1$. Several experimental methods, including NMR spectroscopy, electron microscopy, fluorescence spectroscopy, dynamic light scattering and small angle neutron scattering, indicate that disc-shaped objects are formed in such lipid-detergent mixtures (Glover et al., 2001b; Luchette et al., 2001).

The use of bicelles has been reported to have several advantages compared to micelles. For instance, the integral membrane protein diacylglycerol kinase retains its activity in bicelles, in contrast to micelles (Sanders and Landis, 1995). Furthermore, the membrane protein bacteriorhodopsin refolds in both DMPC/CHAPS and DMPC/DHPC bicelles (Booth et al., 1996, 1997). In addition, the interaction of the HIV-1 envelope peptide with micelles induces a strong curvature in this model membrane, which is not observed in the case of bicelles (Chou et al., 2002).

The versatility of isotropic bicelles as membrane models has been explored further by introducing different lipids in the bicelles. For instance, lipids with different charges on their headgroups, e.g., DMPG and DMPS, have been successfully introduced into bicelles (Struppe et al., 2000). Lipids containing longer fatty acyl chains, such as DPPC or POPC, have been employed to investigate different aspects of peptide-membrane mismatch (Whiles et al., 2002b; Chou et al., 2004). Bicelles also have been reported to form stable crystals with the membrane protein bacteriorhodopsin, allowing X-ray crystallographic studies (Faham and Bowie, 2002).

Lately, another interesting model membrane, referred to as nano-discs, has been developed (Bayburt and Sligar, 2002; Sanders et al., 2004). These discs are very similar to bicelles, except that that the lipid bilayer region is capped by amphipathic peptides instead of detergent molecules.

2.3 Peptides

The distinction between a peptide and a protein is not strictly defined, often depending on the circumstances. One major difference is that proteins usually are larger and often fold into a tertiary structure, whereas peptides only have secondary structure. Another typical feature of peptides is that their structure changes in response to different environments. For instance, a peptide might be an unstructured monomer in solution, but take on a well-defined structure when bound to a membrane. In the present context peptides will be considered to be rather short polymers of amino acids with no specific tertiary structure. Typical secondary structural elements of such polymers are α-helices and β-sheets, which are stabilized by characteristic patterns of backbone hydrogen bonding. However, secondary structures may be discussed more generally as the distributions of ϕ and ψ angles along the backbone.

Even though many peptides exhibit stable structures, considerable motion is still present, both of the whole peptide, but also locally around bonds and side-chains. This motion is often of key importance for the function of the peptide. In some cases these dynamics can be predicted from the structure, but it has been shown that in certain cases dynamic differences can explain differences in function even when the structure appears to be unchanged (Mäler et al., 2000).

The interplay between the structures and dynamics of molecules is often described in terms of energy landscapes, where each possible conformation of a molecule is defined by its energy. In this model, molecular dynamics is represented as fluctuations between the different conformations within this landscape. This energy landscape model can be thought of as a modern expansion of the classical theory of chemical kinetics that predicts that the activation energy is coupled to the rates of chemical reactions (Frauenfelder et al., 1991).

Peptides may position themselves in various ways in a membranous environment, depending both on their aa sequence and, on the properties of the membrane, such as fatty acyl chain length, head-group properties and packing. Two characteristic features of such positioning are: the angle of the peptide relative to the normal of the membrane, and the depth of penetration into the bilayer. Another important aspect in this connection is the length of a hydrophobic stretch of aa compared to the thickness of the hydrophobic core of the bilayer. If these distances are unequal, hydrophobic mismatch can occur.

This mismatch may involve the peptide either being too long (positive mismatch) or too short (negative mismatch), both of which situations influence the membrane lipids and the positioning of the peptide within the membrane. If the hydrophobic region of the peptide is somewhat too long, accommodation might occur by stretching the lipids somewhat, thereby decreasing flexibility (Killian, 2003). However, if it is far too long, the peptide might tilt relative to the membrane normal. On the other hand, if the peptide is too short, it might cause the lipids to become less ordered or else the peptide might position itself perpendicular to the membrane normal.

2.3.1 Naturally occurring peptides

Even though proteins are the primary machines of the cell, peptides are also abundant in nature and exhibit a vast and exciting functional repertoire. For instance, several peptides are used for defensive or offensive purposes, including the antimicrobial peptides of several animals and the peptide-based poisons produced by, for example, bees, wasps and cobras. Other peptides are utilized for signaling in multicellular organisms, both along neural and endocrine pathways. Furthermore, covalently attached to proteins certain peptides serve as tags for sorting within the cell and usually are cleaved off after the targeting of the protein has been completed.

Motilin

Motilin is a peptide hormone whose sequence of 22 amino acids has been determined for at least 10 vertebrate species. Multiple alignments reveal that it is the N-terminal region that is conserved primarily (Figure 7). Site-directed mutagenesis and switching of the amino acid stereochemistry from L to D have confirmed that this region of the molecule is functionally most important (Boulanger et al., 1995).

Homo sapiens (human)	**FVP**I**FT**YGELQRMQ**E**K**E**RNKGQ
Macaca mulatta (rhesus monkey)	**FVP**I**FT**YGELQRMQ**E**K**E**RSKGQ
Oryctolagus cuniculus (rabbit)	**FVP**I**FT**YSELQRMQ**E**R**E**RNRGH
Cavia porcellus (domestic guinea pig)	**FVP**I**FT**YSELRRTQ**E**R**E**QNKRL
Felis catus (cat)	**FVP**I**FT**HSELQRIR**E**K**E**RNKGQ
Sus scrofa domestica (domestic pig)	**FVP**S**FT**YGELQRMQ**E**K**E**RNKGQ
Bos taurus (bovine)	**FVP**I**FT**YGEVRRMQ**E**K**E**RYKGQ
Ovis aries (sheep)	**FVP**I**FT**YGEVQRMQ**E**K**E**RYKGQ
Equus caballus (horse)	**FVP**I**FT**YSELQRMQ**E**K**E**RNRGQ
Gallus gallus (chicken)	**FVP**F**FT**QSDIQKMQ**E**K**E**RNKGQ

Figure 7 Alignment of the amino acid sequences of motilin from 10 vertebrate species. Conserved residues are highlighted in bold.

The biological functions of motilin in humans are indicated by its primary expression in the gut and the nervous system, including the brain (Itoh, 1997). In the gastrointestinal tract, motilin stimulates the contraction of smooth muscles. Its function(s) in the brain and nerve cells remains unclear, although a possible role as a neuro-transmitter has been proposed (Itoh, 1997).

The effects of motilin in the gastrointestinal tract are mediated by binding to a specific receptor, which has recently been cloned and characterized (Fieghner et al., 1999) and found to belong to the large family of G-protein-coupled membrane receptors (GPCR). It is thought that motilin first interacts with the membrane in which this receptor is located prior to binding to the receptor itself (Backlund, 1995). It seems likely that this binding to the membrane induces changes in the secondary structure and molecular dynamics of motilin, as well as orienting this peptide with respect to the receptor, in such a way that recognition is facilitated (Sargent and Schwyzer, 1986).

Extensive biophysical characterization of motilin in various membrane-mimicking media has been performed. Employing ^{1}H-NMR, the structure of this peptide in a solution of 30% HFP (Kahn et al., 1990; Edmondson et al., 1991) as well as in the presence of SDS-micelles (Jarvet et al., 1997) has been determined. In both of these media motilin is primarily α-helical, but with an N-terminal β-turn. Characterization by circular dichroism (CD) indicates that virtually no change in the secondary structure of motilin is induced by vesicles with zwitterionic lipids as compared to motilin in solution, whereas negatively charged lipids induce the α-helical structure (Backlund et al., 1994).

The molecular dynamics of motilin have been studied both by NMR (Allard et al., 1995; Jarvet et al., 1996) and fluorescence spectroscopy (Backlund and Gräslund, 1992; Backlund, 1995; Damberg et al., 2002). In the case of the NMR studies the dynamics were calculated on the basis of relaxation data for the $^{13}C^{\alpha}$-$^{1}H^{\alpha}$-spin vector in the amino acid residue Leu10, revealing that motilin is more rigid in the presence of a membrane mimic, indicating formation of a more stable structure. Characterization of the dynamics of the natural fluorofor Tyr7 in motilin performed by fluorescence anisotropy decay (FAD) indicates that two local correlation times (0.4 ns and 1.7 ns) and one global correlation time (3.6 ns) are required to account for the dynamics of motilin in an aqueous solution of HFP. The overall rotational correlation times determined by FAD and NMR were similar under the same conditions.

2.3.2 Cell-penetrating peptides

The term cell-penetrating peptides (CPPs) is used to refer collectively to peptides that can enter living cells in an apparently receptor-independent manner, most of which are not naturally occurring. The original observations on entry of peptides into fixed cells proved to be artifactual since the fixing procedure itself leads to such uptake (Lundberg and Johansson, 2002). Thus, several presumptive CPPs that have been exhaustively studied do not enter living cells, and thus are not actually CPPs.

In this context the major focus of biophysical interest has been on the mechanism by which a peptide can translocate across a biomembrane. Accordingly, major efforts have been invested in attempts to demonstrate the translocation of peptides across model membranes *in vitro* (Thorén et al., 2000, 2004; Persson et al., 2001, 2004; Drin et al., 2001). The original belief was that the translocation of CPPs should be energy-independent. However, since most of these peptides are positively charged, a membrane potential could act as a driving-force (Terrone et al., 2003), but how this process may occur is not yet understood.

More recently, endocytosis has been proposed as a mechanism for the cellular uptake of CPPs (Magzoub and Gräslund, 2004). However, even if a peptide can be internalized into the cell in an endocytotic vesicle, the problem of membrane translocation remains since the content of such a vesicle is still separated from the rest of the cell by a specialized region of the plasma membrane.

Another important feature of CPPs is their toxicity. It has been proposed that such peptides can be used to introduce foreign substances, e.g., drugs, into cells. However, if the peptide itself is toxic, this approach becomes problematic.

Penetratin

Penetratin, one of the CPPs first identified, originates from a helical segment present in a class of DNA-binding transcription proteins called Homeodomains (Derossi et al., 1994). Determination of the sequence of penetratin (RQIKIWFQNRRMKWKK) revealed that seven of its sixteen amino are positively charged, which is significant in connection with its binding to biological membranes, many of which are negatively charged. Even though eukaryotic plasma membranes are generally neutral overall (Matsuzaki, 1999), the high density of positive charges in penetratin might be crucial for its translocation of specific regions across such membranes. Furthermore, in the light of the high degree of diversity in the membrane lipids the attraction of this peptide to negatively charged domains might be important for its translocation.

Studies indicate, as expected, that penetratin interacts more strongly with vesicles composed of lipids with negatively charged headgroups, than with zwitterionic lipids (Magzoub et al., 2001). Furthermore, the structures of penetratin can vary greatly, depending on the charge density of the membrane with which it interacts (Magzoub et al., 2002). As evaluated by CD spectroscopy with low levels of negatively charged lipids a random structure dominates; at intermediate levels, formation of an α-helical structure is induced; and in the presence of high lipid charge density the structure of penetratin is dominated by β-sheets.

Characterization of the fluorescence quenching of the natural fluorofores in this CPP, i.e., the two tryptophan residues, has revealed that this peptide resides at the surface of both partially and fully negatively charged lipid membranes (Magzoub et al., 2003). The fluoresence depolarization of DPH, which resides in the fatty acyl region of the bilayer, provides an estimate of the influence of a peptide on membrane fluidity. Penetratin does not affect this depolarization, neither in neutral nor partially negatively charged membranes (Magzoub, 2004), indicating a lack of interference with the fatty acyl chains. This conclusion is reinforced by NMR studies on the interaction of penetratin with bicelles containing 30% negatively charged lipids, which show the structure of the peptide to be largely α-helical in good agreement with CD data (Lindberg et al., 2003).

Transportan

Transportan is an artificial chimeric CPP, composed of the 12 N-terminal amino acids residues of the neuroendocrine peptide galanin linked to the wasp venom peptide mastoparan via a lysine residue, to give the sequence GWTLNSAGYLLGKINLKALAALAKKIL. Clearly, transportan contains far fewer positive charges than penetratin, suggesting a different type of membrane interaction, at least in the presence of negative charges. The structure of transportan in vesicles formed from both zwitterionic and partially negatively charged lipids is mainly α-helical, as evaluated by CD spectroscopy (Magzoub et al., 2001). The structure induced by interaction with neutral lipids is slightly less α-helical in character. When the fluoresence of the tryptophan residue in transportan was exploited to examine its position in the membrane, in analogy to the investigation with penetratin described above, this CPP was also found to reside at the membrane surface (Magzoub et al., 2003). However, NMR characterization of transportan in SDS micelles by NMR

provides a less clear indication of the position of this peptide in a model membrane (Lindberg and Gräslund, 2001).

2.3.3 Prion proteins

The discovery of prion proteins has led to a paradigm shift in our understanding of the mechanisms of pathogenesis (Prusiner, 1982, 1997). The long-prevailing idea that the spread of infectious disease always involves delivery of primary genetic material, i.e., DNA or RNA, into a host has been challenged by the existence of this interesting class of molecules.

The prion proteins exist in two forms, i.e., the natural non-toxic form native to the cell and the pathogenic scrapie form. The current hypothesis is that the scrapie form induces disease directly, by altering the conformation of the native prion proteins in the cell. Thus, these proteins can act as catalysts that transform the cells' own proteins into potentially lethal forms.

The underlying mechanism is an area of intensive research interest. From a biophysical perspective this idea challenges Christian Anfinsen's classic idea that a given primary sequence invariably folds to produce the same tertiary structure (Anfinsen, 1973; Dobson, 2003). Moreover, the mechanism of catalysis, and the pathogenesis of the scrapie form are of considerable medical interest and importance as well. One leading hypothesis is that the pathogenesis is coupled to aggregation of the protein in its β-sheet conformation, as is the case with other so-called amyloid-forming proteins.

Bovine prion protein peptide 1 - 30

The function(s) of the native prion protein is presently unknown, but it is thought to be a membrane protein (Hegde et al., 1998). The N-terminal sequence of this protein acts as a signal peptide, or more specifically a nuclear localization (NLS) like signal, to target it to specific membranes for insertion or redistribution. When targeting has been completed this sequence is normally cleaved off, but in infected cells, prion proteins which retain their signal sequences have been observed. It has been speculated that this signal sequence might be involved in the pathogenic process, perhaps serving as a membrane anchor (Hegde et al., 1999; Ott and Lingappa, 2004).

The amino acid residues at the N-terminal of the bovine prion protein have the sequence MVKSKIGSWILVLFVAMWSDVGLCKKRPKP. CD investigations have revealed that this peptide (bPrPp) adopts an α-helical upon interaction with uncharged vesicles, whereas introduction of 30% negatively charged lipids leads to a higher degree of β-sheet structure (Magzoub, 2004). The depolarization of DPH fluoresence in both neutral and partially charged membranes to which bPrPp is bound reveals a clear influence on the fluidity of the interior of the membrane.

3. BROWNIAN MOTION OF MOLECULES

Thermally induced movements in molecules involve a wide range of time-scales and amplitudes. The difference in the time required for formation of the transition state of a chemical reaction and the spontaneous unfolding events that occur with certain proteins can vary from femtoseconds to several days. Not only do the rates of these motions differ by several orders of magnitude, but the underlying processes are often fundamentally different in nature. For instance, the oscillatory motions of bond vibrations are qualitatively different from the random diffusion of molecules in solution. In this chapter the rotational and translational diffusion of whole molecules, as well as intramolecular motions will be discussed. These motions are stochastic, or Brownian, in their nature.

3.1 Rotation and translation

A sphere, which is one of the simplest models for a molecule demonstrates two types of movement: rotation and translation. In an equilibrium liquid state these two modes of motions are random in character, meaning that, for instance, the speed and direction of the translational motion for the molecule may vary considerably at different moments.

The translational diffusion of a sphere is described by the diffusion constant D_{transl}, according to the Stokes-Einstein equation:

$$D_{transl} = \frac{kT}{6\pi\eta r} \tag{2}$$

where k is Boltzmann's constant, T the temperature, η the viscosity and r the radius of the sphere. One way to approach translational diffusion is to consider the average time it requires for this molecule to diffuse a distance d. This time, τ_{transl}, which is one example of a correlation time, is given by the equation:

$$\tau_{transl} = \frac{d^2}{2nD_{transl}} \tag{3}$$

for diffusion in n dimensions.

The second type of overall motion of a sphere is rotation, which can be quantitated as a typical rotational correlation time. This time is defined as the average time it takes for the molecule to rotate through one radian, which is given by the equation:

$$\tau_{rot} = \frac{4\pi r^3 \eta}{kT} \tag{4}$$

with the parameters being defined as in the case of equation (2).

The treatment considerations above relate to ideal spheres but real molecules often have highly complicated shapes. The influence of shape is discussed in the following section. Another complication is the fact that water molecules tend to

adhere to objects such as peptides and lipid aggregates, thereby creating a hydration layer that makes the objects larger and decreases their rate of diffusion. This effect is often corrected for by introducing the radius of hydration, which is the radius of the object under study plus its hydration layer. In practice, the thickness of the hydration layer varies somewhat, but has been estimated to be approximately 3 Å (Halle and Davidovic, 2003).

One important aspect of the diffusional properties of macromolecules is illustrated by the folding of proteins. In the folded state a protein is very dense, but in its unfolded state, for instance, the molten globular state, the protein chains mix more with the solvent molecules, resulting in a larger radius. This implies that the relationship between the mass of a polymer and its translational and rotational properties depends strongly on its physical state (Flory, 1969; Wilkins et al., 1999). However, peptides have been found to be too small to be affected by this phenomenon (Danielsson et al., 2002).

Translational diffusion is also affected when the concentration of large solute molecules is high, since these large particles hinder free diffusion. The ratio between the apparent diffusion coefficient (D) and the unobstructed diffusion coefficient (D_0) may for spherical particles be expressed as in the equation (Söderman et al., 2004):

$$\frac{D}{D_0} = \frac{1}{1 + \frac{\phi}{2}\left(1 + \frac{r}{R}\right)^3} \tag{5}$$

where ϕ is the volume fraction of obstructing particles, R the radius of the obstructing particles and r the radius of the investigated particle. Interestingly, equation (5) predicts a different obstruction of the translational diffusion for the solvent, compared to the large particles. In the limit where $r = R$, this expression is to a first approximation given by the equation:

$$\frac{D}{D_0} = 1 - 2\phi \tag{6}$$

3.2 Anisotropic rotation and translation

In principle molecules may have almost any shape imaginable, due to the large variations in their structures. In practice, however, this fact is often highly inconvenient and simplified models of shape are therefore introduced. One such simplification is to consider the shape as a simple three-dimensional object, which can be defined by the length of its three orthogonal axes. Unfortunately, even this approximation often turns out to be insufficient, since it can be difficult to determine the relative length of all three axes, when two of these are rather similar (Lakowicz, 1999).

Consequently it is often assumed that the shape of a molecule is axially symmetric, i.e., that two of the three axes are equal in length. This gives rise to three situations: when the unique axis is longer than the other two, a prolate (cigar-shaped) object is obtained; when all of the axes are equal in length, the object is a simple sphere; and when the unique axis is shorter, the object is oblate (disc-shaped). These different types of objects exhibit different translational and rotational properties.

The translational diffusion time is modified by a shape factor, *F*, according to the equation:

$$D_{transl} = \frac{kT}{6\pi\eta rF} \tag{7}$$

The size of this shape-factor depends on the type and degree of anisotropy associated with the object in question. Perrin calculated these shape factors for both the rotational and translational motion of ellipsoids, expressing the shape factor for the translation of an oblate as:

$$F_P = \frac{\sqrt{(a/b)^2 - 1}}{(a/b)^{2/3} \cdot \arctan\sqrt{(a/b)^2 - 1}} \tag{8}$$

where *a/b* is the ratio between the length of the long, equal axes, *a*, and that of the short axis, *b* (Perrin, 1934, 1936; Cantor and Schimmel, 1980). Similar expressions have also been developed for the shape dependence on the obstruction of translational diffusion due to large solutes at high concentration (Simha, 1940; Cantor and Schimmel, 1980).

In the case of rotational motion, an axially symmetric object may rotate around either its long or its short axis. These two modes are defined by rotational diffusion coefficients (D_{rot}) where $D_{\parallel}$ is the frequency of rotation around the unique axis (i.e., the short axis in an oblate object) and $D_{\perp}$ the frequency around one of the two axes of equal length (i.e., the long axes in an oblate object) (Woessner, 1962; Lee et al., 1997). This type of motion may also be described in terms of rotational correlation times. Somewhat unexpectedly there are three rotational correlation times, $\tau_1 - \tau_3$, involved according to (Woessner, 1962), i.e.,

$$\frac{1}{\tau_1} = 6D_{\perp} \tag{9a}$$

$$\frac{1}{\tau_2} = \left(5D_{\perp} + D_{\mathrm{II}}\right) \tag{9b}$$

$$\frac{1}{\tau_3} = \left(2D_{\perp} + 4D_{II}\right) \tag{9c}$$

3.3 Time-correlation functions

In the previous sections of this chapter correlation times for rotational and translational motions were discussed. The correlation time describes how rapidly orientational or positional information is lost in connection with random motions. This time-dependent loss of orientational or positional information can be described mathematically by a time-correlation function, one example of which is the auto-correlation function:

$$C(t) = \langle y(t_0) \cdot y(t_0 + t) \rangle - \langle y(t_0) \rangle \cdot \langle y(t_0 + t) \rangle \qquad (10)$$

A mathematically more explicit example of such a time-correlation function is the exponentially decaying time-correlation function:

$$C(t) = e^{-t/\tau} \qquad (11)$$

with the correlation time τ.

It should be pointed out that the time-correlation functions described by equations (10) and (11) are general, i.e., do not describe specific molecular motions. Nevertheless, these equations can be applied to many molecular situations. For instance, the time-correlation function for the rotation of an axially symmetric object is given by the equation:

$$C(t) = A_1 \cdot e^{-t/\tau_1} + A_2 \cdot e^{-t/\tau_2} + A_3 \cdot e^{-t/\tau_3} \qquad (12)$$

where $A_1=(3\cos^2\theta-1)^2/4$, $A_2=3\sin^2\theta\cos^2\theta$ and $A_3=(3/4)\sin^4\theta$, and τ_i is provided by equation (9). θ is the angle between a given bond vector and the unique axis of the object.

The rotation of an entire molecule is not the only rotational motion that occurs. Indeed, rotation around bonds is ubiquitous and occurs on several different time-scales. Within the stochastic limit, such local motion also may be described in terms of time-correlation functions. The rotational motion of a given bond vector thus depends both on the overall motion and on the local motion. If these motions are statistically independent, i.e., occur on very different time-scales, then the observed correlation function is simply the product of the correlation function for the overall motion and the correlation function for the local motion:

$$C_{OBS}(t) = C_{overall}(t) \cdot C_{local}(t) \qquad (13)$$

Local motion is often very restricted in nature, i.e., certain orientations of a bond vector relative to a given molecular frame are impossible. As a consequence of this limitation the local correlation function does not decay to zero, but to a value, S^2. S, referred to as the generalized order parameter, thus provides a measure of the restriction of the local motion. An S value of 1 is associated with a completely immobile vector, while and $S = 0$ describes totally unrestricted motion. The time-correlation function for the restricted motion is described by the equation

(Wennerström et al., 1974; Halle and Wennerström, 1981; Lipari and Szabo, 1982a-b):

$$C_{local}(t) = (1 - S^2) \cdot e^{-t/\tau} + S^2 \qquad (14)$$

Order parameters are important not only when considering restriction of local motion, but also in connection with the order of a liquid crystal. The physical difference between an isotropic and an anisotropic liquid reflects the fact that in the former all orientations of a particle are equally probable, whereas in an anisotropic liquid, certain orientations are more probable. The order parameter of a liquid crystal is related to the degree of anisotropy in the system. More generally, this parameter is related to both the average order of the sample (S_{order}) and the local restriction of motion (S_{local}) the observed order parameter is obtained according to (Seelig, 1977):

$$S_{OBS} = S_{order} \cdot S_{local} \qquad (15)$$

3.4 Time-correlation functions of lipids in membranes

The motions of lipids in membranes, discussed briefly in section 2.1 can also be described in terms of correlation functions. However, due to the multitude of motional modes occurring in a membrane, these functions tend to be very complex. Still, it is possible to create simplified models by extending the reasoning underlying equations (13) and (14). One approach is to divide the motion of lipids in the membrane (in our case, the bicelle) into three different components, i.e., the overall rotation $C_{bicelle}(t)$, lipid motion $C_{lipid}(t)$ and local motion $C_{local}(t)$, producing an overall correlation function, $C_{overall}(t)$, of the type:

$$C_{overall}(t) = C_{bicelle}(t) \cdot C_{lipid}(t) \cdot C_{local}(t) \qquad (16)$$

The apparent overall motion of a bicelle, $C_{bicelle}(t)$, involves two different types of motion, overall rotation and lateral diffusion, where lateral diffusion is the two-dimensional motion of lipids in the transverse plane of the model membrane and is defined in a manner analogous to regular rotational motion. The time required for, e.g., a lipid molecule to diffuse one radian along a vesicle ($\tau_{lat\text{-}rot}$) is given by the time it takes to diffuse the distance equal to the radius of the sphere ($\theta = 1$). The rotational correlation time for lateral diffusion in spheres can therefore be defined as (Bloom et al., 1975):

$$\tau_{lat-rot} = \frac{r^2}{6D_{lateral}} \qquad (17)$$

The observed rotational correlation time for the bicelle is thus given by:

$$\frac{1}{\tau_{bicelle}} = \frac{1}{\tau_{rot}} + \frac{1}{\tau_{lat,rot}} \qquad (18)$$

A lipid molecule in a membrane is free to rotate around its principal axis but the rotation around the other two axes is strongly restricted by the membrane surface. In order to accurately describe its motion, an order parameter for the entire lipid molecule, S^2_{lipid} , is required. This concept is the same for the local motion. Accepting these assumptions, the overall correlation function will have the form (Ellena et al., 1993):

$$C_{overall}(t) = e^{-t/\tau_{bicelle}} \cdot \left(\left(1 - S^2_{lipid}\right)e^{-t/\tau_{lipid}} + S^2_{lipid}\right) \cdot \left(\left(1 - S^2_{local}\right)e^{-t/\tau_{local}} + S^2_{local}\right) \quad (19)$$

By assuming that there is a large difference in the timescale of these three types of motions, (19) can be simplified to obtain:

$$C_{overall}(t) = S^2_{lipid} \cdot S^2_{local} \cdot e^{-t/\tau_{bicelle}} + \left(1 - S^2_{lipid}\right) \cdot S^2_{local} \cdot e^{-t/\tau_{lipid}} + \left(1 - S^2_{local}\right) \cdot e^{-t/\tau_{local}} \quad (20)$$

4. SPECTROSCOPY

In this chapter, the information that is provided by studying the interaction of light with molecules is discussed, in particular the three techniques NMR, EPR and CD spectroscopy.

4.1 Nuclear magnetic resonance - NMR

Atoms, which are the building blocks of molecules, consist of nuclei with surrounding electrons. Both the nucleus and the electrons have four fundamental properties: mass, charge, electric/magnetic shape and spin. Mass, charge and shape can be understood from experiences in everyday life but spin is a rather intangible quantity. Spin is a magnetic property of the particle, and thus interacts with magnetic fields.

Since electrons in the orbitals of atoms or molecules tend to pair up with an electron of the opposite spin, few molecules exhibit a net electron spin. Nuclei are different in this respect, since pairing of nuclear spin does not occur to the extent as with electrons. This fact is exploited in connection with NMR spectroscopy, where the interaction between nuclear spins and a magnetic field is examined.

As interesting as all this is, it is even more exciting that spins tend to influence one another through so-called couplings. There are two types of couplings for a spin of 1/2, the dipole-dipole coupling and the J-coupling. The direct dipole-dipole coupling is observed between spins that are located close to one another. J-coupling is observed for nuclear spins that are coupled by common electrons, i.e., electrons shared in a common molecular orbital and thus involved in covalent bonding.

In addition to the effects of couplings, observed NMR spectra are influenced by another important feature, the so-called chemical shift, which reflects an interaction between a nuclear spin and its surrounding electron cloud (orbitals). A strong external magnetic field induces currents in electronic orbitals, which in turn induces a magnetic field that affects the nuclear spin. The three interactions mentioned so far all involve nuclear spins with net spin not equal zero. In addition there is a fourth interaction that only occurs with spins greater than 1/2. As opposed to nuclei with a spin of 1/2, nuclei with larger spins possess a magnetic shape that can interact with the surrounding electron cloud.

One extremely important feature of NMR spectroscopy is its low sensitivity. This reflects the fact that at room temperature the different energy levels are almost equally populated and, since what NMR measures in practice is the difference between the two energy states (at least in the case of spin = 1/2), the signal obtained is very weak. Even though recent improvements in the instrumentation recently have been dramatic, high concentrations of samples are still required.

Since the experimental portions of this thesis involve standard methodologies, neither the details nor theory of NMR spectroscopy will be discussed here.

4.1.1 Relaxation and dynamics

NMR is basically sensitive to molecular motion occurring on three different time-scales, i.e., pico-nanoseconds, micro-milliseconds, and periods longer than seconds. In order to be able to look into these different time windows, NMR spectroscopists have developed various tools. The motions considered here occur primarily within the pico-nanosecond time-scales, i.e., motions that influence NMR-relaxation.

The relaxation theory applicable to NMR on solutions is in most cases described by the Bloch-Wangsness-Redfield (BWR) theory (Wangsness and Bloch, 1953; Redfield, 1957, 1965). With this approach, relaxation is inferred by treating molecular motion as a stochastic perturbation of the nuclear spins, which are described quantum mechanically via the spin-Hamiltonian. This theory is complex and obscured by a number of mathematical transformations. However, the primary outcome is that relaxation of a given statistical quantum state is dependent mainly on the real part of the spectral density function, which is a function of frequency. A spectral density function is the Fourier transform of a time-correlation function (compare with section 3.3) and can be interpreted physically as the distribution of motional frequencies that influence relaxation. Of course, one very important aspect of the BWR theory is its limitations. This theory is based on a number of assumptions concerning the relationship between the relaxation parameters and molecular dynamics. One guideline concerning limits of the BWR theory is that the relaxation time measured should be much longer than the correlation time that dominates the relaxation (Slichter, 1978). This criterion is often met in connection with NMR studies on molecules in solution, but frequently is no longer fulfilled when paramagnetic agents are introduced, since such agents typically demonstrate much shorter relaxation times. This is a matter of major concern in connection with EPR spectroscopy (compare with section 4.2).

In more physical terms, the theory of NMR relaxation concerns how non-equilibrium spin states are eliminated by molecular motion. The most obvious example of this is the FID (Free Induction Decay, the NMR signal), which decays with a characteristic time, T_2. However, there are usually numerous other relaxation times as well depending on the complexity of the system or the investigative strategy. In this section only three relaxation constants, T_1,T_2 and the steady state NOE (*ssNOE*) will be discussed.

T_1 is often referred to as the longitudinal relaxation constant, since it describes the relaxation of spin-flips, which are thought to occur along the direction of the strong magnetic field. T_2, referred to as the transverse relaxation time constant, is associated with the destruction of statistical spin coherences. Both of these constants reflect auto-relaxation and are always present, even with an isolated spin.

The *ssNOE* relaxation coefficient only exists for dipole-dipole coupled nuclei. This coefficient is not a relaxation time, but rather an enhancement/reduction factor proportional to the cross-relaxation phenomenon, which is caused by a double flip of a spin pair. These effects of spin-flips, i.e., T_1 and cross-relaxation (in the shape of *ssNOE*), can be visualized in an energy diagram (Figure 8).

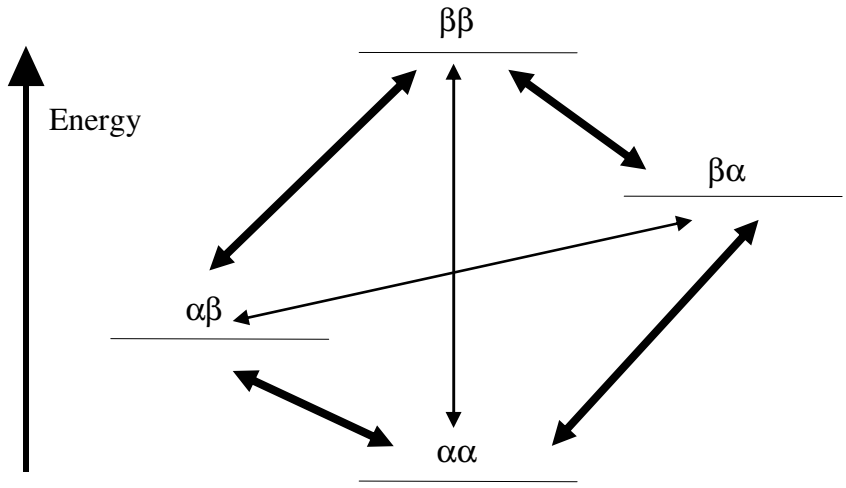

Figure 8 An energy diagram depicting a dipole-dipole coupled spin-pair. The thick lines indicate single-flip transitions (T_1 auto-relaxation) and the thin lines double-flip transitions (cross-relaxation).

In connection with solution-state NMR, relaxation processes are dominated by strong anisotropic (orientation-dependent) interactions. For nuclei with spin of ½, the dipole-dipole coupling and the anisotropic component of the chemical shift (CSA) dominate these interactions. In the case of a heteronuclear spin-pair (typically ^{1}H-^{13}C or ^{1}H-^{15}N), relaxation processes are described theoretically by the BWR theory, in which the T_1, T_2 and *ssNOE* relaxation times are given as linear combinations of the spectral density functions at different frequencies, as follows:

$$\frac{1}{T_1} = R_1 = \frac{d^2}{4}\left[J(\omega_H - \omega_X + 3J(\omega_X) + 6J(\omega_H + \omega_X)\right] + c^2 J(\omega_X) \qquad (21a)$$

$$\frac{1}{T_2} = R_2 = \frac{d^2}{8n}\left[4J(0) + J(\omega_H - \omega_X) + 3J(\omega_X) + 6J(\omega_H)\right] + \frac{c^2}{6}\left[3J(\omega_X) + 4J(0)\right] \qquad (21b)$$

$$NOE = 1 + \frac{d^2 \gamma_H T_1}{4\gamma_X}\left[6J(\omega_H) - J(\omega_H - \omega_X)\right] \qquad (21c)$$

where d is the dipole-dipole interaction constant, c the CSA interaction constant and the n the number of protons attached to nucleus X. The constants c and d are provided by the equations:

$$d = \frac{\mu_0 h \gamma_H \gamma_X}{8\pi^2 r^3} \qquad (22a)$$

$$c = \frac{\omega_X \Delta\sigma}{\sqrt{3}} \qquad (22b)$$

where μ_0 is the vacuum permeability, h Planck's constant, r the distance between the proton and the X nucleus, $\Delta\sigma$ the CSA (which, in general, is assumed to be axially symmetric), γ the magnetogyric ratio and X denotes the heteronucleus of interest, e.g., ^{13}C or ^{15}N.

As can be seen from these formulae the measurement of one of these relaxation constants in a given magnetic field provides information concerning the spectral density function at several frequency points. The spectral density function can be characterized fully by measuring a sufficient (and correctly chosen) number of relaxation constants and calculating the J values at different frequencies, employing a system of linear equations. This method, often referred to as "Spectral Density Mapping" (Peng and Wagner, 1992), has, indeed been applied. However, complete as it is, this approach is rather tedious, since it involves measurement of six relaxation constants and interpretation of the spectral density, which is not always straightforward.

The alternative approach commonly referred to as the 'model-free' interpretation of relaxation data (Wennerström et al., 1974; Halle and Wennerström, 1981; Lipari and Szabo, 1982a-b) can in a sense be considered as mapping the time-correlation function. This model is 'free' in the sense that it involves no physical assumptions concerning how a bond vector moves and is thus in principle applicable to any correlation function. With this model mathematical expression of the time-correlation function provides parameters that may describe the motion, compare with equations (13) and (14). The standard procedure in the model-free approach is to measure T_1, T_2 and the *ssNOE*, although many other relaxation rates/coefficients would do equally well.

The spectral density function of the standard model-free assumptions is obtained from the equation:

$$J(\omega) = \frac{2}{5}\left(\frac{S^2\tau_{overall}}{1+\omega^2\tau_{overall}^2} + \frac{(1-S^2)\tau}{1+(\omega\tau)^2} \right) \qquad (23a)$$

where

$$\tau = \frac{\tau_{overall} \cdot \tau_{local}}{\tau_{overall} + \tau_{local}} \qquad (23b)$$

$\tau_{overall}$ is the rotational correlation time for the entire object, S^2 the generalized order parameter for local motion and τ_{local} the rotational correlation time for this local motion. The parameters resulting from the model-free analysis are reasonably easy to understand in physical terms, at least in comparison to the spectral density function. The spectral density function defined by equations (23) can be extended to include several order parameters and correlation times, if the data measured require application of a more complicated model (Clore et al., 1990; Ellena et al., 1993).

One important feature of the T_2-relaxation rate is its dependency on the spectral density function at zero frequency, J(0). This implies that motions considerably slower than the regular relaxation time-scales influence the value of T_2. Furthermore, adiabatic motions also affect this relaxation time, so that dynamics that do not cause energy transitions may influence T_2. For instance, the T_2 values are

influenced by fast chemical exchange motion, lasting from micro- to milliseconds and implying a fast exchange rate (k_{ex}) according to:

$$k_{ex} >> \Delta\omega \tag{24}$$

where $\Delta\omega$ (s^{-1}) is the difference between chemical shifts in the NMR signals from the two conformations, A and B, and k_{ex} is the exchange rate (s^{-1}). In more chemical terms, k_{ex} is defined as the sum of two rate constants that describes the exchange according to:

$$A \underset{k_2}{\overset{k_1}{\rightleftharpoons}} B \tag{25}$$

where $k_{ex} = k_1 + k_2$. The average T_2 value observed for the two readily interchanging conformations can be calculated according to (McConnell, 1958):

$$\frac{1}{T_{2,average}} = \frac{p_A}{T_{2A}} + \frac{p_B}{T_{2B}} + \frac{p_A p_B \Delta\omega^2}{k_{ex}} \tag{26}$$

where k_{ex} is the exchange rate (s^{-1}) and p_X the probability of state X. Thus, the average T_2 becomes dependent on the square of the strength of the magnetic field ($\Delta\omega^2$) under fast interchanging conditions, which exist when the probabilities of the two conformations are of the same magnitude. In the expression for T_2 provided by equation (21b) this dependence on $\Delta\omega^2$ can be inferred from the phenomenological term R_{ex}.

The molecular dynamics derived from NMR relaxation studies discussed here have focused on the motion of a single bond vector, as is usually the case for analysis of the dynamics of peptide backbones. It should, however, also be mentioned that other types of motion, such as the dynamics of amino acid side-chains, may be examined employing modified relaxation methodologies (Millet et al., 2002; Skrynnikov et al., 2002).

4.1.2 Translational diffusion

NMR spectroscopy can also be employed to determine translational diffusion through the use of pulsed magnetic field gradients (PFG), typically performed as a gradient spin-echo experiment. By increasing the gradient strength or delay-times step-wise, it is possible to calculate the translational diffusion time, D_{transl}, according to the Stejskal-Tanner equation (Stejskal and Tanner, 1965):

$$I = I_0 e^{-\gamma^2 g^2 \delta^2 D_{transl}\left(\Delta - \frac{\delta}{3}\right)} \tag{27}$$

where I is the peak intensity, I_0 the intensity without gradients, g the pulsed field gradient strength, γ the magnetogyric ratio, Δ the T_2 delay time and δ the T_1 longitudinal storage period.

These measurements are straightforward for simple systems, but become more complicated for systems characterized by fast chemical exchange or target molecules or complexes of different sizes. In the case of fast chemical exchange, aspects of relaxation come into play if the two states exhibit different transversal and longitudinal relaxation rates. Methods to overcome these problems have been developed, for example, by measuring values at several delay times and thereafter extrapolating to a delay time of zero.

At the same time, fast exchange is not a problem only since the translational diffusion measurements can, in fact, be used to calculate the sizes of the populations in the two conformations (A and B) (Lindman et al., 1984). If one of the states can be measured separately, the populations, p, of the two states can be calculated according to

$$D_{OBS} = p \cdot D_A + (1 - p) \cdot D_B \qquad (28)$$

where D_i are translation diffusion coefficients. This approach is very useful for studies of complex formation and, if the concentrations of all the species are known, can be employed to calculate binding constants.

4.1.3 Positioning in the membrane

Several approaches allow information concerning the position of peptides or proteins in model membranes to be obtained from the NMR signals of either the peptides or the lipids. A classical procedure in this connection involves measurement of the quadrupolar splittings of ^{2}H-labeled lipids in an ordered membrane matrix. The quadrupolar coupling is dependent on orientation, and the observed splitting, Δ, is provided by:

$$\Delta = \frac{3}{2}\left(\frac{e^2 qQ}{h}\right) S_{CD}\left(\frac{3\cos^2\theta - 1}{2}\right) \qquad (29)$$

where e is the elementary charge, q the charge of the proton (+1), Q the nuclear quadrupolar moment, h Planck's constant, S_{CD} the order parameter for the ^{2}H-^{13}C spin vector and θ the angle between the director and the external magnetic field (Seelig, 1977). (Qe^2q/h), which is often referred to as the quadrupolar coupling constant, is influenced by the electrical surroundings of the ^{2}H nucleus. In order to interpret the order parameter it is helpful to compare equation (29) with equation (15), in which $S_{OBS} = S_{CD}$.

Thus changes in quadrupolar splittings induced by a peptide can be interpreted in terms of alterations in local ordering of the lipids. One possible interpretation is that an increase in the order parameter reflects an enhancement of positive hydrophobic mismatch (Bloom et al., 1991), i.e., the hydrophobic stretch of amino acids in the peptide is longer than the width of the hydrophobic lipid region (compare with section 2.1). Accordingly, a decrease in the order parameter would indicate a

negative hydrophobic mismatch (shorter peptide) or that the peptide is located in some way at the surface.

Another approach to examining the positioning of peptides in membranes is through the addition of paramagnetic agents, e.g., paramagnetically labeled lipids (Figure 9) or paramagnetic ions (such as Mn^{2+} or Gd^{3+}), and determination of their effects on the NMR signals observed from the peptide.

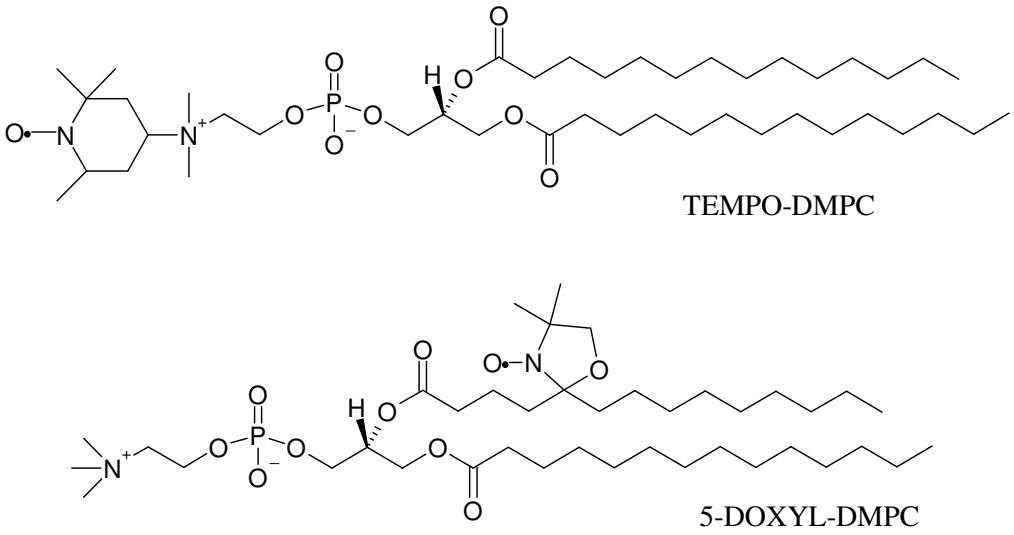

Figure 9 DMPC molecules containing the two spin labels TEMPO (attached to the headgroup) or DOXYL (attached to carbon five in the *sn2* chain).

The reverse procedure, i.e., adding of a spin labeled peptide to the membrane, can also be informative. Such addition of paramagnetic agents may either broaden the peaks, and/or shift peak positions in the spectrum. The broadening effects represent in principle relaxation experiments, in which the NMR signals are affected by the paramagnetic relaxation mechanism. The advantages of this procedure over observations of quadrupolar splittings are that it can be performed in isotropic systems and that the position of the peptide in the membrane can be determined in greater detail. The major drawback is that the addition of large spin labels may perturb the system.

A third indication of the positioning of a peptide in a membrane can be obtained from the secondary $^1H^N$ shifts of the peptide (Wishart and Sykes, 1994). Positive $^1H^N$ secondary shifts are typical for regions exposed to a hydrophobic environment whereas regions exhibiting negative shifts are generally exposed to hydrophilic environments. Although this method is not as direct as the two other procedures discussed above, it can be highly useful, since it gives indications of membrane positioning simply from assigning the peaks in a spectrum.

A standard method for examining peptide positioning in membranes is measurement of the kinetics of exchange of peptide protons with solvent deuterons, or vice versa. Such measurements provide information concerning which parts of the peptides are hidden in the membrane. However, this approach has one serious drawback namely, that the exchange rates for protons in highly structured regions are

also much slower. Thus, it can be difficult to distinguish between regions involved in H-bonding, e.g., α-helices and β-sheets, and regions that are buried in the membrane.

4.1.4 Structure

The fact that the dipole-dipole coupling is dependent on distance allows inter-nuclear distances to be determined from these couplings. As discussed in section 4.1, the dipole-dipole averages out in solution. Nonetheless, it still remains as a mechanism of relaxation, but is effective only over distances of less than 5 - 6 Å. This fact is not only a problem, but also a blessing. If much longer couplings could also be observed, each pair of nuclear spins would give rise to a cross-peak and the NOESY spectrum would become too crowded to be interpretable.

Other ways to measure distances by NMR have involved systems where the dipole-dipole coupling does not average out to zero. Recent advances in the development of recoupling dipole-dipole couplings in solid-state magic-angle spinning (MAS) experiments have made it possible to determine structures of proteins in frozen samples (Castellani et al., 2002). Another interesting development is the measurement of 'residual' dipolar couplings in a weakly anisotropic liquid phase (Tolman et al., 1995; Tjandra and Bax, 1997).

The structures investigated here have all been solved by classical isotropic state ^{1}H-methods, so that the subsequent discussion will focus solely on this methodology. It should, however be pointed out that much more structural information can be obtained by labeling the peptide with ^{13}C and/or ^{15}N and the use of sophisticated solution-state pulse sequences (Cavanagh et al., 1996).

The three fundamental two-dimensional experiments that provide the basis for homo-nuclear structural determination by NMR are COSY (Aue et al., 1976), TOCSY (Braunschweiler and Ernst, 1983) and NOESY (Jeener et al., 1979). The COSY and TOCSY approaches make use of the J-coupling for magnetization transfer, whereas NOESY is based on the Nuclear Overhauser Effect (NOE). The NOE is dependent on the remnants of the dipole-dipole coupling in the liquid state and thus represents a relaxation phenomenon.

The practical difference between COSY and the TOCSY experiments is that the former provides information only about covalently bonded spin-pairs that are no more than three bonds apart. In the case of TOCSY all spin pairs within a system that are J-coupled, such as in the side-chain of an amino acid, can be observed. This is due to the fact that TOCSY induces potent J-coupling in the system, which is normally observed only in the solid state.

The type of (and number of) peaks that can be observed by NOESY and TOCSY is fine-tuned by a mixing time in the pulse sequence. Several variants of these basic experiments have been developed for increasing spectral quality as well as for determining molecular parameters such as J-couplings. The basic steps involved in solving the structure of a small to medium sized molecule, such as a peptide or a small protein, using homonuclear NMR are as follows (Wüthrich, 1986):

1. Assignment of a large number of ^{1}H resonances in the molecule through the use of COSY, TOCSY and NOESY. On the basis of these assignments, it is then possible to obtain indications of secondary structural elements by calculating secondary chemical shifts (Wishart and Sykes, 1994).

2. Measurements of NOESY peak, which provides information on ^{1}H-^{1}H distances. Information concerning torsion angles can be derived from the J-couplings observed via the Karplus equation (Karplus, 1959).
3. From the connectiveties, distances and torsion angle constraints, obtained a family of structures are calculated. From these structures that converge, the most favorable ones are considered to represent the structure

An extremely important aspect of structures determined by solution-state NMR techniques is that they are, in fact, solved in solution. This is in strong contrast to X-ray crystallography and electron diffraction methods, where the molecules of interest must be arranged in a very highly ordered crystal. Even though enzymatic activity has been observed in such crystals (Bränden and Tooze, 1999), it is clear that crystallization can give rise structural artifacts.

Lately, it has been shown that inclusion of data on molecular dynamics, for instance, generalized order parameters, in NMR structural calculations improves the structural precision (Lindorff-Larsen et al., 2005). As mentioned previously, however, structural determination by solution-state NMR is limited to short distances. For longer distances, other spectroscopic methods, such as electron paramagnetic resonance (EPR) come into play (Borbat et al., 2001). The long-distance structural information provided by a paramagnetic probe can be included in structural NMR studies. The usefulness of this approach has been demonstrated by the determination of the structure of the α-helical transmembrane protein mistic (Roosild et al., 2005).

One major obstacle to structure determination by solution-state NMR has been the limitation to molecules of relatively small size, due to the dependence on rotational correlation times. Recently, however, a modification of the standard HSQC pulse-sequence, TROSY, has extended the applicability of solution-state NMR techniques to much larger objects (Pervushin et al., 1997).

4.2 Electron paramagnetic resonance - EPR

Electron paramagnetic resonance (EPR) or electron spin resonance (ESR) is a spectroscopic technique closely related to NMR, in which unpaired electrons are detected. Such electrons are either present in paramagnetic ions or free radicals, and these species are rather uncommon, at least in comparison to the occurrence of nuclei with spin $\neq 0$. The EPR spectrum has features similar to those of an NMR spectrum. For instance, the EPR g-value is similar to the NMR chemical shift and the isotropic g-value differs in different environments.

Due to the scarcity of unpaired electrons, electron spin-spin couplings are rarely observed by chance. On the other hand couplings between electron spins and nuclear spins, so-called hyperfine couplings, are frequently seen and may be considered to be J-couplings between nuclear and electronic spins. One example of such hyperfine-coupling is the coupling between the radical electron in a typical spin-label and the nearby ^{14}N nucleus (Figure 9). Since the nucleus of ^{14}N has a spin of 1, this coupling gives rise to a triplet in the EPR spectrum (Figure 10).

The motion of a spinlabel strongly affects the appearance of the EPR spectrum. This is because the T_2 relaxation of the spinlabel is sensitive to rotational motion. The time-scale of the dynamics for the spinlabel is often divided into fast and slow motions. A fast motion is typically characterized by reorientational correlation times of less than ~ 3 ns (Grell, 1981). If the motion of the spin-label is restricted in some fashion, order parameters may also affect the shape of the spectrum. The

appearance of the EPR spectrum is thus influenced both by the motional time-scale, and on restriction of motion, making it possible to extract motional parameters from such a spectrum (Figure 10). It is thus possible to estimate, for instance, order parameters for the spin-label by measuring linewidths of the EPR spectrum (Berliner, 1976).

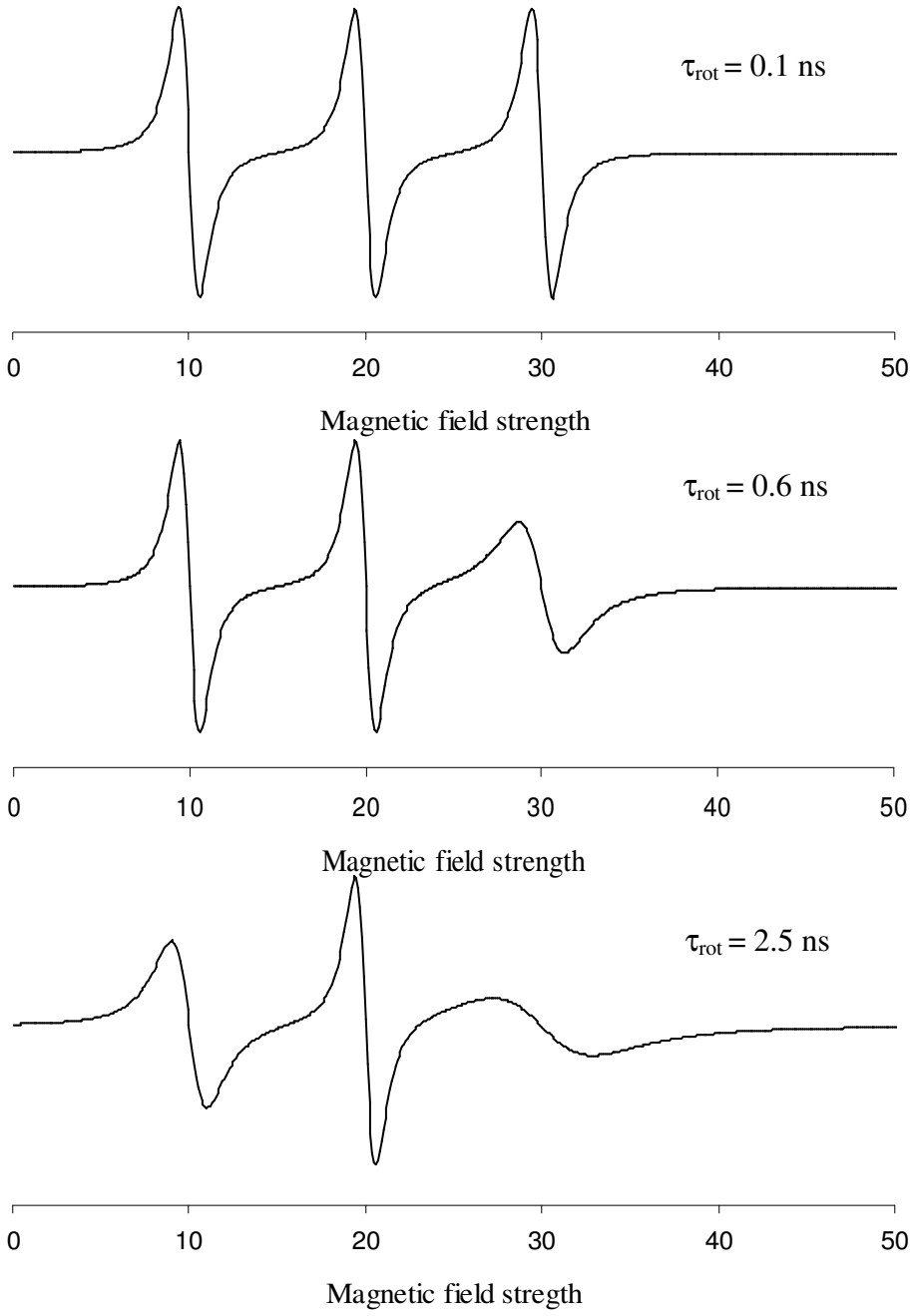

Figure 10 Three calculated EPR spectra indicating the influence of the overall rotational correlation times of the spin-label on line broadening (adapted from 'Biological spectroscopy' by (Campbell and Dwek, 1984)).

4.3 Circular dichroism - CD

Light is an electromagnetic wave that may rotate either to the left or to the right along the direction of the translational motion. One interesting aspect about these two rotational states is that they interact differently with chiral molecules, and since many biological molecules are chiral, for example, almost all of the amino acids in cells are L-stereo isomers; CD spectroscopy is a useful tool for studying these molecules. What kinds of information can be extracted from the CD spectrum of a peptide? Since the interaction of far-UV light with the backbone amide moieties in peptides is dependent on the ϕ and ψ angles in the backbone, different secondary structural elements give rise to typically different CD spectra. Accordingly, the CD spectrum of a peptide or protein is analyzed by comparison with characteristic spectra of, for example, α-helices and β-sheets (Figure 11).

However, it is very rare that such a spectrum exhibits only a single secondary structural motif. In the case where two characteristic structures are present, there is an isochroic point, i.e., a point at which the spectral intensity does not change upon changing conditions, such as the temperature. Thus, observation of such a point can provide valuable information. Analysis of the CD spectra of more complicated systems is difficult. Attempts to interpret complicated spectra simply as linear combinations of typical spectra have been made, but care should be taken in this connection since CD spectra are in principle not additive (Glatti et al., 2002).

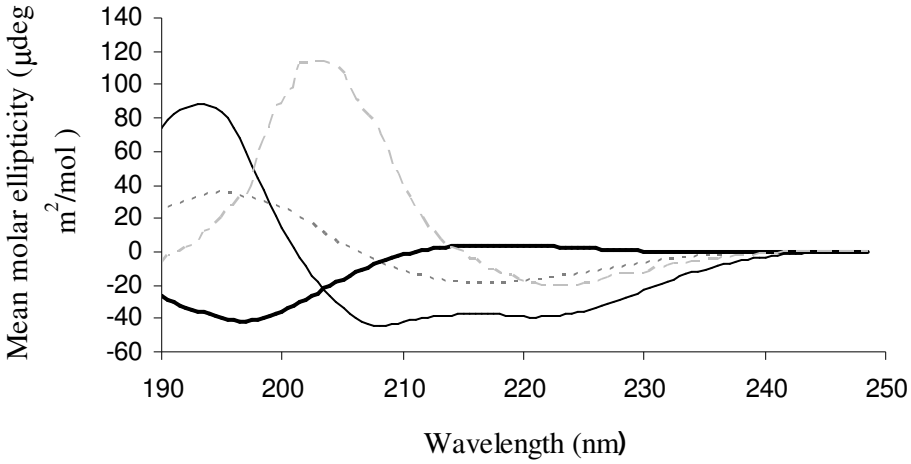

Figure 11 The characteristic CD spectra obtained with four secondary structures. The thick black line represents a random coil, the thin black an α-helix, the long stripes parallel- and short stripes anti-parallel β-sheets.

Part 2: Discussion

5. RESULTS AND DISCUSSION

Disc-shaped assemblies of lipid/detergent molecules were observed in bile as early as in the mid 1960's (Small et al., 1966, 1969; Small, 1967). These particular discs contain mixtures of phosphatidylcholines and bile salts. At the end of the 1970's, similar artificial mixtures of lipids and bile salt analogues (e.g., CHAPS and CHAPSO) were examined by Mazer an co-workers (Mazer et al., 1980) who reported that that the disc-shape concept was complicated by the mixing of these two components. By the end of the 1980's Roberts and coworkers (Bian and Roberts, 1990; Lin et al., 1991) were investigating DMPC/DHPC mixtures which also were found to be disc-shaped.

Around this same time, Sanders and coworkers characterized both DMPC/CHAPSO mixtures (Sanders and Prestegard, 1990) and, later, mixtures of DMPC/DHPC (Sanders and Schwonek, 1992). In 1988, Ram and Prestegard found that lipid/bile-salt mixtures can be induced to form ordered phases in strong magnetic fields (Ram and Prestegard, 1988). The macroscopic ordering of these mixtures was later exploited by Bax and collaborators to study dissolved molecules and to measure residual dipole-dipole couplings (Tjandra and Bax, 1997). By the end of the 1990's both anisotropic and isotropic mixtures of DMPC and DHPC were being utilized as versatile model membrane systems by Vold and coworkers (Vold and Prosser, 1996; Vold et al., 1997; Struppe et al., 2000). Now, at the beginning of the second millennium, the usefulness of bicelles as model membranes is being explored by several research groups.

In the second part of this thesis the experimental results, presented in publications I - VI will be discussed and compared to relevant literature reports. This discussion is divided into a number of important questions concerning the properties of bicelles as model membrane.

5.1 How large are the bicelles?

The sizes of molecules and molecular aggregates can be determined by a large number of methods. However, as discussed in chapter 3, several other molecular characteristics, including the shape, dynamic state (e.g., folding/unfolding), aggregation and size distributions, must also be considered in interpreting the results obtained. Depending on the method used, different sets of parameters come into play and in many cases, for instance, the shape of a given object must be assumed in order to estimate its size.

The approach presented here involves PFG-based NMR measurements of translational diffusion, as discussed in section 4.1.2. The translational diffusion of bicelles is described in papers II, III, V and VI. The interpretation of translational diffusion data on bicelles in terms of size relies on the fact that it is possible to measure the diffusion of the entire aggregate.

Since the solubility of a typical lipid in water is very low (~ 10^{-10} M (Evans and Wennerström, 1999)) the diffusion of DMPC most certainly reflects the bicelle diffusion. Fortunately, two of the lines in the ^{1}H NMR spectrum of DMPC/DHPC bicelles arising from the methyl groups in the fatty acyl chains, do not overlap (Figure 13) (Vold et al., 1997). In the case of DMPC/CHAPS bicelles, almost none of these lines overlap.

Another important aspect of the determination of the overall size of bicelles from diffusion data might be contributions from lateral diffusion of DMPC in these bicelles. However, it can be argued, on the basis of the size of the bicelles (see also below) and the time typically required to dephase the NMR signal of these structures that this lateral diffusion accounts for < 1% of the observed diffusion. The translational diffusion coefficients for bicelles without peptides are documented in Table 3.

Table 3 Translational diffusion constants for bicelles at 37 °C, as determined by ^{1}H PFG NMR.

		D_{transl} ($\cdot 10^{-11}$ m^2s^{-1})			
Paper	Solvent	DMPC/DMPG	DHPC	CHAPS	H_2O/HDO
II	[DMPC]/[DHPC] = 0.5[a]	2.1	4.6	-	234
II	(0.7·[DMPC] +0.3·[DMPG])/[DHPC] = 0.5[a]	2.2	4.9	-	231
V	[DMPC]/[DHPC] = 0.5[b]	2.9	5.5	-	ND[c]
VI	[DMPC]/[DHPC] = 0.25[b]	7.3	9.7	-	251
VI	[DMPC]/[[DHPC] = 0.5[b]	2.7	5.9	-	260
VI	[DMPC]/[CHAPS] = 0.5[b]	5.8	-	6.5	242

a measured in D_2O
b measured in 90% H_2O
c not determined

The rates of translational diffusion of bicelles of different sizes and types exhibit large differences. Bicelles with a [DMPC]/[DHPC] ratio of 0.25 diffuse much more rapidly than bicelles with a corresponding ratio of 0.5, as expected. More surprising is the more rapid diffusion of bicelles with a [DMPC]/[CHAPS] ratio of 0.5, compared to those with [DMPC]/[DHPC] = 0.5. This latter observation might reflect the lower aggregation number of CHAPS micelles (compare with Table 2), rendering CHAPS molecules more effective as detergents.

Another important aspect in this connection is that the miscibility between CHAPS and DMPC may be greater than the miscibility between DHPC and DMPC, rendering the DMPC/CHAPS bicelles less disc-like. Furthermore the difference in rates of diffusion for DMPC and DHPC is larger than for DMPC and CHAPS, implying that a larger proportion of the CHAPS is located in bicelles, making these bicelles smaller on the average. A general observation was that both DHPC and CHAPS diffuse faster than DMPC in all of the samples examined, which probably reflects the presence of a non-bicelle-bound fraction of these detergents (Ottiger and Bax, 1998; Struppe and Vold, 1998; Glover et al., 2001b). Measurement of the concentration-dependent diffusion of DHPC in paper II revealed that the level of this free fraction is below the CMC for this detergent in an aqueous solution.

The diffusion coefficient for water was used as an internal probe for apparent viscosity in the bicelle mixtures. In general, the viscosity of all samples was lower than that of pure water, which is predicted to be approximately $300\cdot10^{-11}$ m^2/s at 37 °C

(Mills, 1973). Recently, Geamers and Bax (Gaemers and Bax, 2001) proposed that the obstruction is a major determinant of viscosity changes in bicelles. However, other factors may also be important, e.g., the influence of free detergent molecules.

As discussed in section 3.1, the diffusion coefficient of an object is related to its size and shape. Expressions relating the thickness of the bicelle to the radii of the long axes have been developed (Vold and Prosser, 1996; Glover et al., 2001b; Triba et al., 2005) on the basis of geometrical arguments concerning the shape of bicelles. In paper VI a novel expression is given that is independent of the shape of the rim region of the bicelle, namely:

$$r = \frac{2qV_{lipid}\sigma a}{b} \tag{30}$$

where r is the radius of the bilayer region, σ the number of detergent molecules bound to the bicelle per unit area, V_{lipid} the volume of one lipid molecule and q the q - ratio. a and b represent the thickness of the fatty acyl region and the full thickness of the bilayer region, respectively. One advantage of this relationship is that it can be used to predict differences in size, of bicelles formed using different detergents, which is important for explaining the differences in diffusion coefficients observed in bicelles with either DHPC or CHAPS.

In order to estimate the size of the bicelles from data on their translational diffusion, relationships of the type described by equation (30) are utilized to calculate a frictional shape factor. The most common assumption is that bicelles exhibit an approximately oblate shape, so that the Perrin shape factor can be employed. This approach was applied in paper V to calculate the radius of bicelles with a [DMPC]/[DHPC] ratio of 0.5.

The shape of bicelles is, however, expected to be more cylindrical than ellipsoidal and accordingly a cylindrical shape factor should be utilized. Unfortunately, no analytical expressions for the dependence of the diffusion of a cylinder whose equal axes are longer than the odd axis on friction have been developed. Consequently, it is difficult to obtain any reasonable values for the size of the bicelles.

However, in order to make comparisons with other methods, it is possible to calculate an apparent radius of hydration using the Stokes-Einstein's equation (2). For a DMPC/DHPC bicelle with q = 0.5, the radius of hydration can be calculated to be 78 Å, using D_{transl} = $2.9 \cdot 10^{-11}$ m^2s^{-1}, T = 310 K and η = 10^{-3} ms^{-1}. However, since bicelles are relatively large, at high concentration the diffusion of a given bicelle is hindered by the presence of other bicelles.

Therefore, in order to correctly interpret the data an obstruction factor is also required. By assuming a spherical shape equation (6) can be utilized, and by employing a typical volume fraction of bicelles (ϕ = 15 %), the obstruction effect turns out to be 0.7. Interpreting this factor, the apparent radius of hydration for the bicelle with q = 0.5 becomes 55 Å. A major problem associated with this calculation is that the obstruction factor itself is also inherently dependent on the size and shape of the object.

Another important influence on the size of bicelles is the miscibility of the lipids and detergents as has been discussed recently by Triba and co-workers (Triba et al., 2005). This phenomenon can readily be introduced into equation (30): if p is the relative population of DMPC in the bilayer region, s the relative population of DHPC

in the rim region, V_{det} the volume of one detergent molecule and δ the number of lipid molecules per unit area, the following expression is obtained:

$$r = \frac{2aV_{DMPC}V_{DHPC}\left(qs\sigma - (1-p)\delta\right)}{b\left(pV_{DHPC} - q(1-s)V_{DMPC}\right)} \qquad (31)$$

The derivation of this equation, for the slightly more general case of ellipsoidal bilayer regions, is presented in the Appendix.

NMR studies on the translational diffusion of isotropic bicelles have recently been conducted by other research groups as well. The diffusion coefficient for bicelles with a [DMPC]/[DHPC] ratio of 0.3 has been reported to be $6.2 \cdot 10^{-11}$ m^2/s at 25 °C (Wang et al., 2004) a value which agrees well with our findings on bicelles with q = 0.25 (Table 3). A diffusion rate of $5.3 \cdot 10^{-11}$ m^2/s at 22 °C for bicelles with q = 0.5 was observed by Marcotte and co-workers (Marcotte et al., 2004), which indicates the presence of a much smaller bicelles in their system than what we report in papers II, III, V and VI. Their measurements were presumably performed using a mixture of DMPC and DHPC signals, which results in overestimation of the diffusion coefficients of the bicelles. Furthermore, it is not clear whether isotropic bicelles exhibit the same morphology above and below the $L_\beta \rightarrow L_\alpha$ transition temperature of DMPC. Chou and co-workers (Chou et al., 2004) calculated the translational diffusion of bicelles with a [DMPC]/[DHPC] ratio of 0.15 to be $9.2 \cdot 10^{-11}$ m^2/s at 27 °C, which is in good agreement with the diffusion obtained for bicelles with q = 0.15 bicelles in the presence of the peptide penetratin (Table 4).

The size of bicelles has also been determined using other approaches. Dynamic light scattering resulted in smaller values of the size of the bicelles with a [DMPC]/[DHPC] ratio of 0.5, i.e., r = 32Å (van Dam et al., 2004) and r = 36 Å (Glover et al., 2001b). Employing neutron scattering techniques, the size of the same bicelles was estimated to be slightly larger, i.e., r = 43 Å (Luchette et al., 2001). The deviation of these values from the radius of hydration calculated on the basis of NMR diffusion measurements probably reflects the influence of shape and obstruction factors.

5.2 Do the peptides bind to the bicelles?

It is not unreasonable to propose that virtually any peptide will interact with a biomembrane to some extent. Nevertheless, strong binding is indicative that this binding may be associated with function. The binding of peptides to model membranes may be addressed using several experimental approaches which, however, may provide answers that differ both qualitatively and quantitatively. For instance, monitoring the induction of structure in a peptide as a measure of its interaction with a membrane may be very tricky, since the structure may not actually change upon binding. Moreover, this method is very difficult to quantitate.

Investigations on translational diffusion can provide a quantitative measure of the binding of a peptide to a biomembrane (compare with section 4.1.3). Therefore, in papers II, III and V the translational diffusion constants for the peptides motilin, penetratin and bPrPp in bicellar solution were measured by means of NMR and the resulting data are summarized in Table 4.

Table 4 Diffusion coefficients for the peptides motilin, penetratin and bPrPp in the absence and presence of bicelles containing DMPC/DHPC or (DMPC + DMPG)/DHPC

		D_{transl} ($\cdot 10^{-11}$ m^2s^{-1})			
Paper	Peptide	Mixture	DMPC/DMPG	peptide	H_2O/HDO
II	motilin	3mM buffer	-	21.1	253
II	motilin	q = 0.5	2.8	6.1	230
II	motilin	q = 0.5, 30% DMPG	2.6	4.7	235
III	penetratin	3 mM in buffer	-	28	329
III	penetratin	7.5 mM in buffer	-	26.3	316
III	penetratin	10 mM in buffer	-	26.1	317
III	penetratin	q = 0.5	2.5	2.7	270
III	penetratin	q = 0.5, 30% DMPG	1.9	2.4	280
III	penetratin	q = 0.15, 30% DMPG	9.4	10.3	280
V	bPrPp	q = 0.5	2.6	-	-

These translational diffusion data for both motilin and penetratin in the presence and absence of bicelles reveal clearly that both of these peptides interact with the bicelles, i.e., their diffusion is slower in a bicellar solution. In the case of motilin this effect is more pronounced when 30 % of the DMPC is replaced by the negatively charged DMPG. Using equation (28), it is possible to calculate that 84% of the motilin binds to the neutral bicelles and 90% binds to the partially acidic bicelles.

The diffusion of penetratin in solution was found to be concentration dependent, indicating that this peptide is prone to aggregate, thereby rendering estimation of its binding to bicelles difficult. Nonetheless, it is clear that penetratin does interact with partially negatively charged bicelles. The observation that penetratin also interacts with neutral bicelles is surprising, since other studies indicate that this should not be the case (Magzoub et al., 2001, 2002, 2003). For instance, blue shifts in fluoresence emission of the two tryptophan residues in this peptide have been observed in the presence of vesicles containing lipids with negatively charged headgroups, but not with neutral vesicles.

In order to compare these findings to the situation in bicelles, the fluoresence of penetratin in our two bicellar systems was measured here (Figure 12, unpublished data).

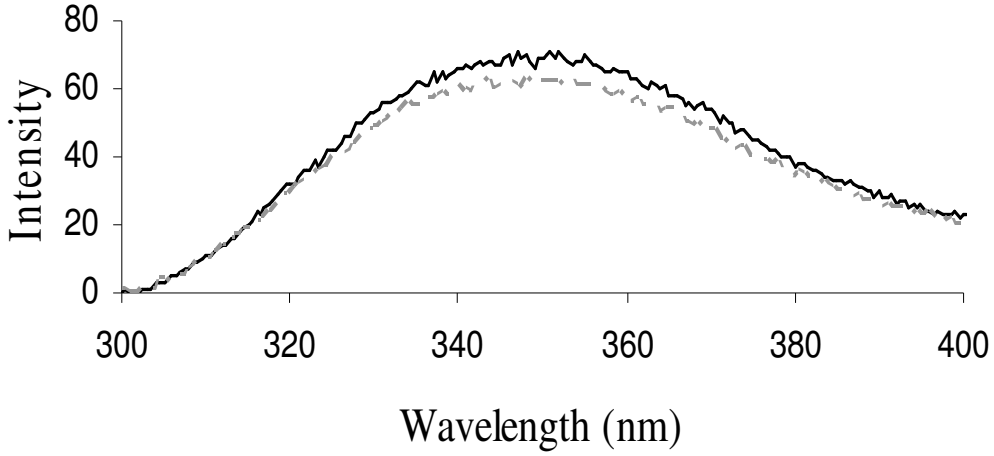

Figure 12 Fluoresence emission spectrum of the two tryptophan residues of penetratin in the presence of neutral (grey) and partially acidic (black) bicelles with q = 0.5.

Since the emission wavelength is the same and the intensity similar for penetratin in both of these bicellar systems, it appears that the interaction of this peptide with these two model membranes is very similar. This conclusion supports diffusion data observed by NMR, but at the same times raises a question whether the membrane environment provided by bicelles differs from that of vesicles.

Comparison of the values in Tables 3 and 4 reveals that the apparent diffusion of the bicelles is altered when motilin is present, in a surprising fashion, i.e., the diffusion constant is increased. This is the case for both partially acidic and neutral bicelles.

Although it is to be expected that when two objects bind, the resulting larger complex should demonstrate a slower diffusion, it is improbable that all of the bicelles in a sample have exactly the same size and shape, and that both size and shape distributions are present. Thus, the addition of a peptide might influence these distributions, causing a shift in the apparent size of the bicelles.

In contrast to motilin, penetratin increases the diffusion of neutral bicelles and reduces these movements of partially acidic bicelles. Of relevance in this context is the finding that aggregation of vesicles containing lipids with negatively charged headgroups is induced by penetratin (Persson et al., 2001; Magzoub, 2004). bPrPp slows down the diffusion of neutral bicelles.

5.3 Why can the NMR signals from molecules interacting with bicelles be observed?

In section 5.1 it was shown that bicelles are rather large objects, even though different methods provide different estimates of their exact size. Assuming that a bicelle with q = 0.5 has a radius of hydration of 40 Å , and that $\eta = 10^{-3}$ kg/ms and T = 37 ^{o}C, we can use equation (4) to estimate that the rotational correlation time for bicelle is 62 ns. If this motion were the only movement exhibited by bicelles, their NMR spectra would be extremely broad and featureless (Figure 13). Since this is not

what is observed experimentally, neither for the lipids nor for attached peptides, other extensive motions within the bicelle must affect the NMR relaxation rates.

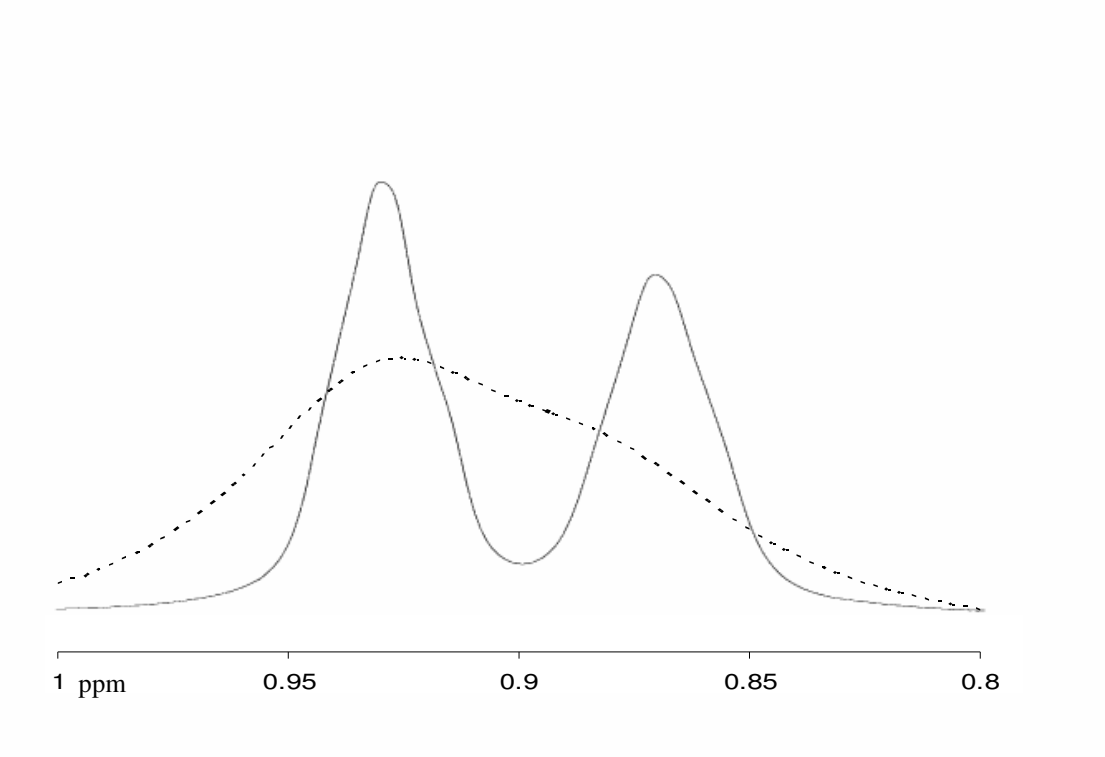

Figure 13 Experimental (continuous line) and simulated (dotted line) ^{1}H spectra of the fatty acyl methyl groups in DHPC (0.93 ppm) and DMPC (0.88 ppm) in a bicelle with q = 0.5 at 37 ^{o}C at a magnetic field strength of14 T. The simulated spectrum was calculated using a rotational correlation time of 62 ns and a proton-proton distance of 2.5 Å.

In order to understand the relationship between size and reorientational motions within the bicelles, relaxation studies were performed on the peptides motilin and penetratin. In paper I a single ^{13}C–labeled α-carbon in the Leu10 residue of motilin was investigated by measuring T_1, T_2 and *ssNOE* relaxation constants at multiple magnetic field strengths. Especially interesting here is the difference in the dynamics of motilin which interacts with neutral or partially acidic bicelles with q = 0.5. Clear differences are observed in the relaxation rates themselves and the standard model-free interpretation demonstrated that the apparent rotational motion of motilin in the presence of neutral bicelles (τ_{rot} = 7 ns) is much faster than in the presence of the acidic structures (τ_{rot} = 14.2 ns). The local motion was also different, with a lower order parameter for the neutral sample (neutral: S^2 = 0.6, acidic: S^2 = 0.69).

These data are clearly different from other reports on similar interactions in other model membranes (Jarvet et al., 1997) (compare with section 2.3.1). Furthermore, this investigation demonstrates that the dynamics of motilin in the bicelle-bound state is clearly dependent on the charge density of the lipid head-groups present, in agreement with the strong binding to both types of bicelles, described in the previous section. The large difference in rotational correlation times does not reflect the size of the bicelles, but rather differences in the motion of motilin within these bicelles.

In paper III the molecular dynamics of penetratin in the presence of bicelles was found to be similar to the dynamics of motilin. In this case, the relaxation of three

^{15}N-labeled sites (Ile3, Ile5 and Phe7) in the backbone was investigated. Even though these bicelles exhibit the same apparent size as the bicelles used in the studies on motilin, different overall rotational correlation times were observed (for Ile3, 19.3 ns; Ile5, 19.4 ns and Phe7, 17.4 ns). Again, it seems that the overall rotation of the peptide does not reflect the overall size of the bicelles.

For penetratin in smaller bicelles, with q = 0.15, shorter overall correlation times were observed (Ile3, 8 ns; Ile5, 7.7 ns and Phe7, 6.9 ns). These values are in better agreement with the expected size of these objects. However, the local dynamics of the peptide in these bicelles are quite different from that of the bicelles with q = 0.5. The average order parameter for penetratin in bicelles with q = 0.5 is S^2 = 0.76, compared with S^2 = 0.51 in the smaller ones. This indicates that the smaller bicelles provide an altogether different environment than the larger bicelles.

This, in turn, raises questions concerning the q-value at which the bicelles form a bilayer region. When Chou and co-workers (Chou et al., 2002) adressed this question by increasing the q-value, they found that no changes in the NMR spectrum of a bicelle-bound apaptide at q-values larger than 0.25. As we shall see, this observation is very similar to what we found for concerning dynamics in bicelles [DMPC]/[DHPC] ratios of 0.5 and 0.25.

Other research groups have also examined the dynamics of peptides in bicelles by NMR relaxation. Whiles and co-workers (Whiles et al., 2001) investigated the relaxation at three sites in the wasp venom peptide mastoparan X in the presence of q = 0.4 bicelles and found that the overall rotation in bicelles containing neutral lipids (8 ns) was slightly smaller than in the case of acidic bicelles (10.6 ns). This phenomenon is very similar to what was observed here for motilin. The order parameters in obtained by Whiles et al. are extremely high (for neutral bicelles S^2 = 0.93; for acidic bicelles S^2 = 0.97), which means that the dynamics of mastoparan X is highly restricted or that measurements at a single magnetic field strength might not be sufficient to allow correct interpretation of the dynamics.

In another study Chou and co-workers (Chou et al., 2004) examined T_1/T_2 ratios of the M2 peptide in the presence of bicelles with q = 0.15 and q = 0.3. In the absence of fast chemical exchange, this ratio provides estimates of rotational correlation times. The overall rotation of M2 was shown to depend on the q - value of the bicelles. The average value for two sites was 25.8 ns for the larger bicelles and 21.5 ns for the smaller ones. However, this dependence does not correlate with the overall size of the bicelles. This conclusion is very similar to what was seen here for motilin and penetratin.

In paper VI the effects of different motional modes of the DMPC molecules in different bicelles are discussed. The dynamics of lipids in model membranes have been extensively studied using NMR relaxation for many years (Bloom et al., 1975, 1991; Brown et al., 1983, 2002; Pastor et al., 1988; Mayer et al., 1990; Halle, 1991; Ellena et al., 1993). For instance, it is well known that the lipids in a membrane do not tumble freely, but that such motion is highly restricted. In order to correctly account for this restriction, order parameters for the entire lipid molecules were introduced.

In paper VI equation (19) was used to model lipid dynamics, in contrast to the peptide dynamics where mainly equations (13) and (14) were used. However, fitting the overall correlation time proved difficult. Since T_2 is the only relaxation parameter measured that is sensitive to slow motions (compare with equation (21b)), the T_2 values was excluded from the fittings, thereby rendering the fitted data independent of the overall rotation of the bicelles, as well as lateral diffusion.

In order to compare the dynamics of lipids in bicelles of different sizes, these measurements were performed on three different bicellar solutions, i.e., [DMPC]/[DHPC] = 0.5, [DMPC]/[DHPC] = 0.25 and [DMPC]/[CHAPS] = 0.5. The dynamics for the ^{13}C-2^{1}H vectors for carbon atoms 2, 3, 12 and 13 (Figure 3) in the fatty acyl chains of DMPC in the bicelles were monitored. A simple comparison of the relaxation data for these different bicelles reveals that that T_2 is the only relaxation parameter that appears to be affected by overall rotation (Figure 5 in paper VI). The dynamics parameters fitted include local order parameters and correlation times for each site and the lipid dynamics in these two types of DMPC/DHPC bicelles were found to be very similar. This supports the assumption that the influence of overall size is decoupled in the analysis.

Judging from the generalized order parameters, the motion in the DMPC/CHAPS bicelles is more restricted (Table 3 in paper VI). This finding is not unexpected, since the molecular structure of CHAPS is rather similar to that of cholesterol (Figure 6) and cholesterol is well known to increase the order of lipids in membranes. It is not unlikely that the pronounced influence of CHAPS on DMPC dynamics reflects, at least in part, a change in miscibility, as discussed in section 5.1. This CHAPS-induced restriction on DMPC dynamics is highly interesting, since it demonstrates that the motion of the lipids is much more affected by the choice of detergent than by the overall size of the bicelles.

In paper VI lipid dynamics were investigated using not only NMR, but also by EPR of spin-labeled lipids. For this purpose DMPC was labeled with the TEMPO spin-label in the headgroup, or a DOXYL group was attached to either the 5th or the 12th carbon atom in the acyl chain (Figure 9). When the order parameters for the spin-labeled lipids in DMPC/DHPC bicelles were calculated from the EPR spectra, the same trends as in the NMR studies were observed: the order parameters in the DMPC/DHPC bicelles are rather similar, whereas the DMPC/CHAPS bicelles are more rigid. Thus, these findings provide qualitative support for the conclusions drawn using NMR. Furthermore, it is clear that the appearance of the EPR spectra as well is largely independent of the size of the bicellar object.

Taken together, these results show that, indeed, extensive motion occurs within the bicelles. Furthermore, the data demonstrate that the NMR T_2 values represent a delicate balance between the overall motion and the motions within the bicelles. This model suggests why transportan gives rise to a ^{1}H NMR spectrum of reasonable quality in the presence of bicelles with q = 0.3, but not in bicelles with q = 0.5. bPrPp exhibits an even stronger dependence on the fluidity in the membrane, since with this peptide spectra of good quality are observed only in DHPC micelles, not in bicelles. This is in clear contrast to motilin and penetratin for which high-quality data could be obtained in bicelles with q = 0.5.

Although the relaxation data for several peptides in bicelles have been successfully fitted employing the standard model-free approach, it is not clear that this is the most physically sound procedure. It is well known that the overall motion of several membrane-interacting peptides within the membrane is restricted. It is therefore not so far-fetched to propose that the same model applied to the analysis of relaxation data for lipids should also be used for the peptides, including an order parameter for the entire peptide.

5.4 Where are the peptides located in the bicelles?

In the previous section it was pointed out that well-resolved NMR spectra could not be obtained for bPrPp in bicelles. Consequently, in paper V the positioning of this peptide was therefore investigated by measuring the quadrupolar couplings for deuterated DMPC lipids in anisotropic phase bicelles with q = 3.5.

The average effect of bPrPp on these splittings is an increase, which is interpreted as an increase in the local order parameter (equations (15) and (29)). Such an increase in local order is often interpreted in terms of positive hydrophobic mismatch and thus predicts a transmembrane configuration of the peptide in which where the transmembrane region of the peptide is slightly longer than the hydrophobic thickness of the bilayer. In the light of the fact that bPrPp contains a rather long stretch of hydrophobic amino acid residues (compare with section 2.3.3) and that its structure is largely α-helical, this result is not very surprising.

However, this interpretation of the ^{2}H-spectra is rather indirect. So, in order to investigate further whether bPrPp resides in a trans-membrane orientation, ^{2}H/^{1}H exchange studies were performed using DHPC-micelles. After 6 hours, all of the $^1H^N$ had exchanged, with the exception of the backbone amide protons in residues 10 - 19, which correspond to the transmembrane α-helical region of the peptide. These observations are consistent with a trans-membrane configuration.

As discussed in section 4.1.3, monitoring the relaxation effects of paramagnetic substances on NMR spectra can provide site-specific information. In paper II the $^1H^\alpha$ - $^1H^N$ region of a TOCSY spectrum of the N-terminal region (residues 1 - 7) of motilin in bicelles was shown to be selectively broadened beyond the limits of detection by the presence of 5-DOXYL labeled lipids (Figure 9). The conclusion that this part of the peptide is inserted into the fatty acyl region of the membrane is supported by the effects of paramagnetic Mn^{2+} ions, which broaden the signals from the C-terminal region.

In paper IV, the positioning of transportan in bicelles revealed a more complicated pattern. The effects of lipids labeled with 5-DOXYL or 12-DOXYL on the TOCSY spectrum indicate a periodical pattern, typical of an amphipathic helix. A similar interpretation was arrived at by analyzing $^1H^N$ secondary shifts. The analysis for transportan in bicelles provided a much clearer picture, than was obtained with SDS micelles (Lindberg et al., 2001). This difference might reflect a general problem concerning the positioning of peptides in micelles. Since it is not clear whether the peptide binds the micelle, or if the detergents bind the peptide, this might perturb the membrane-like qualities of the micelles, especially in terms of membrane positioning.

In conclusion, the three peptides bPrPp, motilin and transportan have different localization within the membrane. bPrPp adopts a transmembrane configuration, the peptide hormone motilin inserts its N-terminal into the fatty acyl region of the membrane and the cell-penetrating peptide transportan adopts a orientation parallel to the surface of the membrane. These differences may well be correlated with different the different biological function s of these peptides, and it shows the importance of being able to accurately determine these properties.

Investigations on the positioning of peptides in bicelles have been carried out by several other research groups as well. One interesting study on the positioning of penetratin in partially negatively charged bicelles (Lindberg et al., 2003) involving the addition of Mn^{2+} ions and 5- and 12-DOXYL-labeled lipids reveal that this peptide resides in the interface between the headgroup region and the hydrophobic core. In a more systematic study, molecular oxygen (which is, indeed, paramagnetic) at high

pressures was used as a probe for the fatty acyl region of the bicelle (Ellena et al., 2003, 2004). Rather than simply measuring paramagnetically induced peak broadening, changes in T_1 were also monitored. Since the distribution of molecular oxygen in lipid bilayers is well characterized, more precise information could be obtained.

In addition, Vold and coworkers (Glover et al., 2001a; Whiles et al., 2001) investigated the orientation of the peptides mastoparan X and the prion protein segment 110 - 136 in large ordered bicelles, by selective ^{2}H-labeling of these peptides. This interesting approach indicated that mastoparan X is oriented perpendicular the membrane normal in neutral bicelles and parallel to the normal in negatively charged bicelles. Moreover, the normal of the helix in the prion protein fragment was found to reside at an angle of 16^{o} relative to the bilayer normal.

Furthermore, the effects of hydrophobic mismatch were investigated employing the model transmembrane peptide P16, in this case by selective ^{2}H-labeling of both the peptide and lipids (Whiles et al., 2002b) with DMPC (14 carbons) and DPPC (16 carbons) as the bilayer lipids, P16 exhibited a transmembrane orientation. However, using DLPC (12 carbons) instead, this transmembrane orientation was lost.

As was shown by investigations on ^{2}H-labeled lipids in ordered bicelles as well as utilizing spin-labels as membrane positioning probes provide valuable insights into membrane/peptide interactions. However, such studies can only be performed on ordered or solid-state type of systems or by introducing perturbing paramagnetic agents. In paper VI the ^{1}H-^{13}C *ssNOE* factors for several sites located in DMPC in DMPC/CHAPS bicelles were determined (Figure 8 in paper VI). It is known for several proteins that the *ssNOE* often correlates quite well with the square of the generalized order parameter, S^2. Upon dissolving the bee venom melittin in bicelles with a [DMPC]/[CHAPS] ratio of 0.5 we observed changes in lipid dynamics reflected in the *ssNOE* factors (Figure 14, unpublished data).

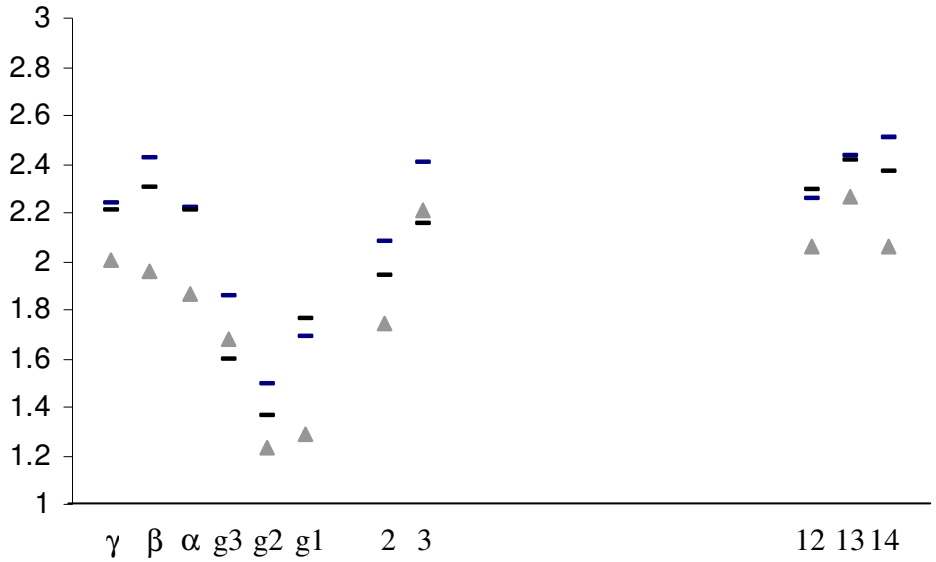

Figure 14 The effect of melittin on the ^{13}C-^{1}H *ssNOE* factors for DMPC in bicelles with a [DMPC]/ [CHAPS] ratio of 0.5. 6 mM melittin was added to 96 mM DMPC at 37 ^{o}C at a magnetic field of 14 T. The effects of melittin are depicted as triangles. For the nomenclature concerning ^{13}C-DMPC, see Figure 3.

It can be seen that the *ssNOE* factors for almost all sites are decreased when melittin is present, which may be interpreted as a stiffening of almost all sites by melittin. This is a typical effect associated with positive hydrophobic mismatch, and indicates that the peptide exists in a transmembrane configuration. This shows that the relaxation-based method presented in paper VI has potential for being used to investigate the position of peptides in bicelles.

5.5 Why are the structures of peptides that interact with membranes of interest?

In papers I, IV and V the structures of the peptides motilin, transportan and bPrPp, respectively, in the presence of bicelles or micelles (bPrPp) have been solved using ^{1}H NMR techniques. All of these peptides were found to be largely α-helical, which was expected both on the basis on their CD spectra, and the structures of a large number of other membrane-interacting peptides. However, considering the large differences in their sequences and biological functions, the reason for these structural similarities is not obvious.

Why these peptides have nearly the same structure and how is this structure related to their putative biological functions? It is reasonable to propose that in these cases the structural similarities are not the key to biological function which could be considered a bit disappointing. However, this leads us to the conclusion that the function of such peptides may be more closely related to other features of their interactions with membranes, such as positioning and molecular dynamics. Indeed, in the previous sections of this chapter the more pronounced diversity in positioning and dynamics of these peptides has been described.

The structure of motilin in the presence of bicelles is rather similar that to observed in HFP and SDS-micelles (Kahn et al., 1990; Edmondson et al., 1991; Jarvet et al., 1997). Although the typical N-terminal β-turn is present in all of these situations, structural details were seen to differ, possibly, at least in part, because different solvents were used. It should be noted that the structures of small peptides might be more sensitive to, e.g., the curvature of a model membrane, than are membrane proteins, which often have a stable tertiary fold.

The structures of several membrane proteins have been solved by applying solution-state NMR techniques to micellar solutions and even more have been elucidated by X-ray crystallography (Torres et al., 2003). However, the number of membrane proteins whose structures are now known is smaller than for soluble proteins, perhaps because of the sensitivity of membrane protein structure to micellar membrane systems. For instance, the interplay between different conformational states and functional dynamics may be strongly influenced by the absence of appropriate lipids, and/or a well-defined bilayer region.

5.6 Are bicelles good model membranes?

Even though bicelles have been studied using numerous approaches, both in the presence and absence of various peptides, much about what these objects is still unknown. For instance, certain peptides might perturb the bicellar morphology, e.g., by making pores, or causing aggregation. It is evident that several peptides can affect the apparent size of bicelles (Table 4) and that peptides may interfere with local lipid dynamics as well (Figure 14). These observations may be important not only for

understanding bicelles, but also for elucidating the mechanism of action of such peptides.

In this thesis, where several peptides have been studied in bicellar solutions, a major question is whether it is possible to draw any conclusions concerning biological function on the basis of these investigations. Papers I and II demonstrated clearly that the peptide hormone motilin interacts differently with negatively charged bicelles compared with neutral bicelles, e.g., binding more strongly to the former. Furthermore, the molecular dynamics of motilin in these two systems differ, with the negative charges both restricting local dynamics and slowing down the motion of the entire peptide in the bicelle down.

Another interesting insight here is the positioning of the well conserved N-terminal region of motilin. Previous studies indicate that it is this region which interacts with the receptor and we show here that this region consists of a β-turn that resides at the interface between the polar headgroup and the fatty acyl regions. Together these observations indicate that motilin may bind preferably to negatively charged domains in the plasma membrane and that the positioning and structure of this peptide in the membrane may facilitate the interaction with the receptor.

In the case of bPrPp, the hypothesis that this segment may act as a membrane anchor seems not unreasonable in the light of the experimental results presented in paper V. Its α-helical structure, in a transmembrane configuration represents a classical membrane-interacting motif.

For the two cell-penetrating peptides penetratin (paper III) and transportan (paper IV) no clear conclusions concerning putative translocation mechanism are obvious from the present results. However, there are similarities in the membrane positioning and structures of these two peptides. Both are largely α-helical and reside in the head-group region of bicelles. The dynamics of penetratin in bicelles of different sizes and SDS micelles differ greatly, indicating that in order to obtain biologically relevant information on peptide dynamics, care must be taken in choosing the membrane model.

Paper VI, in which the dynamics of lipids in bicelles was investigated, reveals that even though lipid motion in a bilayer represent a highly anisotropic system, the NMR relaxation data could be explained sufficiently well employing a simple isotropic model. Local order parameters in bicelles with [DMPC]/[DHPC] ratios of 0.5 and 0.25 were very similar and of the same magnitude as those observed for DMPC in vesicles. Moreover, the degree of order of all of the measured sites in DMPC was significantly higher in bicelles with a [DMPC]/[CHAPS] ratio of 0.5. These conclusions concerning lipid dynamics based on NMR-relaxation investigations were confirmed qualitatively by EPR studies on spin-labeled lipids.

Considered together, these investigations clearly demonstrate that the local lipid dynamics in the bicelles are strongly dependent on the detergent present. Furthermore, the present study shows that it is possible to decouple the local dynamics of the lipids and lipid reorientation from the overall reorientation of the bicelles in the analysis of NMR relaxation data which was also the case for the dynamics of bicelle-bound peptides. An interesting finding from these studies on lipid dynamics in bicelles is that the physical properties of the bicelles can be tuned, not only by the use of different lipids as has been suggested, but also by using different detergents.

In several publications it has been debated whether small isotropic bicelles are actually disc-shaped. The main support for such morphology comes from neutron scattering profiles and electron microscopy (Glover et al., 2001b; Luchette et al.,

2001). Other findings reveal that bicelles possess an apparent radius of hydration larger than associated with DHPC or CHAPS micelles. One fundamental observation is that that high concentrations of lipid employed are actually solubilized by the detergent when making the samples. Altogether, it is clear that the detergent and the lipid molecules actually form aggregates together and it is probable that these aggregates are disc-shaped. However, further investigations on bicellar morphology, especially in the presence of peptides, are required in order to put the field on a more solid ground.

The main reason for using bicelles as model membrane is that they provide a more natural membrane environment than do micelles. However, since far fewer bicellar than micellar systems have been characterized, it is difficult to draw any general conclusions at the present. In the case of micelles, it is well-known that different systems may exhibit radically different properties. SDS-micelles are well known to denature both membrane and soluble proteins. And even though the activity of the membrane protein diacylglycerol kinase is higher in bicelles than in certain micelles, this activity has been found to be even higher in certain mixed micellar systems (Czerski and Sanders, 2000). In contrast, the activity of the peripheral membrane protein phospholipase A is rather similar in several different types of bicelles (Whiles et al., 2002a). These observations lead us to wonder whether the main strength of bicelles is they provide an adequate environment for many peptides and proteins, even though more optimal solutions may exist for each specific case.

Many of the peptide-bicelle interactions examined here appears to be inter-related. The observation that the molecular structure and dynamics of the peptide are altered upon binding to a bicelle is perhaps not very surprising. More interesting are the differences observed with bicelles of different lipid compositions.

Another perspective on the binding of peptides to bicelles is that not only are the physical properties of the peptides modified, but those of the bicelle as well. Several peptides change the apparent size of bicelles and some also alter the local lipid dynamics.

Another exciting observation is that the divergence in the properties of membrane-interacting peptides is more likely to be related to membrane positioning and/or molecular dynamics than molecular structure. Even though at present this is merely a correlation, it might turn out to be a fundamental one. NMR is uniquely suitable for studying, e.g., molecular dynamics and membrane positioning experimentally, and the methodology explored in this thesis might provide unique and important insights into the biological function of several other membrane-interacting peptides as well.

5.7 Future?

The use of bicelles as membrane models has been found to provide new and interesting insights into how peptides interact with membranes. However, many questions remain to be answered and experimental methodology must be developed further in order to answer these questions. One important problem is to resolve the discrepancy between the values of the NMR-derived diffusion coefficients and the estimates of size obtained from scattering experiments. First, it would be interesting to determine these diffusion coefficients by some other technique, for instance, fluoresence correlation spectroscopy (FCS) as well. Secondly, the influence of the

obstruction factor should be estimated, e.g., by measuring the diffusion of the bicelles at several volume fractions.

Another important goal is to improve our understanding of the dynamics of molecules that interact with bicelles. NMR-relaxation investigations on peptides containing several labeled sites might possibly include an anisotropic model, if the bicelle-bound structure is known. Again, it could be rewarding make comparisons with other techniques, e.g., fluoresence anisotropy decay (FAD) measurements on natural peptide fluorofores.

The question as to whether bicelle-interacting peptides reside in the lipid bilayer region or in the detergent rim is also important. A possible experimental approach in this context could be to characterize the influence of adding spin-labeled lipids or detergents on relaxation. Such an experiment could also provide information concerning the miscibility of the lipids and the detergents. Furthermore, it would be highly interesting to characterize the effects of peptides on lipid dynamics in isotropic bicelles, which could be done, e.g., through NMR-relaxation investigations on the lipids and/or EPR studies of spin-labeled lipids.

APPENDIX

In paper VI a model for determining the radius of the bilayer region of a bicelle was developed based on geometrical arguments. Here this model is extended to include the miscibility of the detergents and lipids present. The distances given here are defined in Figure 7 in paper VI. The area of the exposed fatty acyl region of an elliptic disc is given by:

$$A = \pi \cdot a \cdot (c + b) \tag{A1}$$

The volume of the lipid bilayer region of the bicelle is given by:

$$V = \pi \cdot b \cdot c \cdot d \tag{A2}$$

If the number of detergent molecules per units of hydrophobic surface area is given by σ, the total number of detergent molecules in the rim can be calculated from the relationship:

$$n_{\text{det}}^{rim} = \sigma \cdot A \tag{A3}$$

In analogy, the number of lipid molecules in the rim region is defined by:

$$n_{lipid}^{rim} = \delta \cdot A \tag{A4}$$

where δ is the number of lipid molecules per hydrophobic surface area. The total number of lipid molecules in the bilayer region can be calculated from:

$$n_{lipid}^{bilayer} = \frac{V}{V_{lipid}} \tag{A5}$$

where V_{lipid} is the volume of a single lipid molecule. The analogous expression for detergent molecules in the bilayer region is as follows:

$$n_{\text{det}}^{bilayer} = \frac{V}{V_{\text{det}}} \tag{A6}$$

If the relative fraction of lipid molecules in the bilayer region is p ($0 \le p \le 1$) and the relative fraction of detergent molecules in the rim is s ($0 \le s \le 1$),then the q-ratio is provided by:

$$q = \frac{p \cdot n_{lipid}^{bilayer} + (1-p) \cdot n_{lipid}^{rim}}{s \cdot n_{\text{det}}^{rim} + (1-s) \cdot n_{\text{det}}^{bilayer}} \tag{A7}$$

By combining equation (A7) with equations (A1) - (A6), we obtain the relation:

$$q = \frac{p \cdot \frac{\pi bcd}{V_{lipid}} + (1-p) \cdot \pi a(c+d)\delta}{s \cdot \pi a(c+d)\sigma + (1-s) \cdot \frac{\pi bcd}{V_{\det}}} \tag{A8}$$

Upon setting $d = c \cdot z$, equation (A8) is simplified, and the following equation is obtained:

$$q = \frac{p \cdot \frac{bcz}{V_{lipid}} + (1-p) \cdot a(1+z)\delta}{s \cdot a(1+z) \cdot \sigma + (1-s) \cdot \frac{bcz}{V_{\det}}} \tag{A9}$$

This equation can be reformulated, as follows:

$$c = \frac{a(1+z)V_{lipid}V_{\det}(qs\sigma - (1-p)\delta)}{bz(pV_{\det} - q(1-s)V_{lipid})} \tag{A10}$$

When $z = 1$, the circular shape is obtained; while setting $p = s = 1$ yields the non-miscible case.

REFERENCES

Allard, P., J. Jarvet, A. Ehrenberg, and A. Gräslund. 1995. Mapping of the spectral density function of a C^{α}-H^{α} bond vector from NMR relaxation rates of a ^{13}C-labeled α-carbon in motilin. *J. Biomol. NMR* 4:133-146

Anfinsen, C.B. 1973. Principles that govern the folding of protein chains. *Science* 181:223-230

Anlansson, E.A.G., S.N. Wall, M. Almgren, H. Hoffmann, I. Kielmann, W. Ulbricht, R. Zana, J. Lang, and C. Tondre. 1976. Theory of the kinetics of micellar equilibria and qualitative interpretation of chemical relaxation studies of micellar solutions of ionic surfactants. *J. Phys. Chem.* 80:905-922

Arnold, A., T. Labrot, R. Oda, and E.J. Dufourc. 2002. Cation modulation of bicelle size and magnetic alignment as revealed by solid-state NMR and electron microscopy. *Biophys. J.* 83:2667-2680

Aue, W.P., E. Bartholdi, and R.R. Ernst. 1976. Two-dimensional spectroscopy. Applications to nuclear magnetic resonance. *J. Chem. Phys.* 64:2229-2246

Backlund, B.M. 1995. Structural and Dynamical Studies of the Gastrintestinal Petide Hormone Motilin. Doctoral Thesis, Umeå University, Umeå

Backlund, B.M., and A. Gräslund. 1992. Structure and dynamics of motilin. Time-resolved fluorescence of a peptide hormone with a single tyrosine residue. *Biophys. Chem.* 45:17-25

Backlund, B.-M., G. Wikander, T.L. Peeters, and A. Gräslund. 1994. Induction of secondary structure in the peptide hormone motilin by interaction with phospholipid vesicles**.**. *Biochim. Biophys. Acta* 1190:337-344

Bayburt, T.H., and S.G. Sligar. 2002. Single-molecule height measurements on microsomal cytochrome P450 in nanometer-scale phospholipid bilayer disks. *Proc. Natl. Acad. Sci. U. S. A.* 99:6725-6730

Berliner, L.J. 1976. Spin labeling. Theory and Applications. Academic Press, London

Bian, J.R., and M.F. Roberts. 1990. Phase separation in short-chain lecithin/gel-state long-chain lecithin aggregates. *Biochemistry* 29:7928-7935

Bloom, M., E.E. Burnell, A.L. MacKay, C.P. Nichol, M.I. Vlic, and G. Weeks. 1975. Fatty acid chain order in lecithin model membranes determined from proton magnetic resonance. *Biochemistry* 17:5750-5762

Bloom, M., E. Evans, and O.G. Mouritsen. 1991. Physical properties of the fluid lipid-bilayer component of cell membranes: a perspective. *Q. Rev. Biophys.* 24:293-397

Booth, P.J., A. Farooq, and S.L. Flitsch. 1996. Retinal binding during folding and assembly of the membrane protein bacteriorhodopsin. *Biochemistry* 35:5902-5909

Booth, P.J., M.L. Riley, S.L. Flitsch, R.H. Templer, A. Farooq, A.R. Curran, N. Chadborn, and P. Wright. 1997. Evidence that bilayer bending rigidity affects membrane protein folding. *Biochemistry* 36:197-203

Borbat, P.P., A.J. Costa-Filho, K.A. Earle, J.K. Mosciciki and J.H Freed 2001. Electron spin resonance in studies of membranes and proteins. *Science* 291:266-269

Boulanger, Y., A. Khiat, Y. Chen, D. Gagnon, P. Poitras, and S. St-Pierre. 1995. Structural effects of the selective reduction of amide carbonyl groups in motilin 1-12 as determined by nuclear magnetic resonance. *Int. J. Pept. Protein Res.* 46:527-534

Bränden, C., and J. Tooze. 1999. Introduction to Protein Structure. Garland, New York

Braunschweiler, L., and R.R. Ernst. 1983. Coherence transfer by isotropic mixing: applications to proton correlation spectroscopy. *J. Magn. Reson.* 53:535-560

Brown, M.F., A.A. Ribeiro, and G.D. Williams. 1983. New view of lipid bilayer dynamics from 2H and 13C NMR relaxation time measurements. *Proc. Natl. Acad. Sci. U. S. A.* 80:4325-4329

Brown, M.F., R.L. Thurmond, S.W. Dodd, D. Otten, and K. Beyer. 2002. Elastic deformation of membrane bilayers probed by deuterium NMR relaxation. *J. Am. Chem. Soc.* 124:8471-8484

Campbell, I.D., and R.A. Dwek. 1984. Biological Spectroscopy. Benjamin Cummings, Menlo Park

Cantor, C.R., and P.R. Schimmel. 1980. Size and Shape of Macromolecules. Biophysical Chemistry Part II: Techniques for the Study of Biological Structure and Function. Freeman, San Francisco

Carruthers, A., and D.J. Melchior. 1983. Study of the relationship between bilayer water permeability and bilayer physical state. *Biochemistry* 22:5797-5807

Castellani, F., B. van Rossum, A. Diehl, M. Schubert, K. Rehbein, and H. Oschkinat. 2002. Structure of a protein determined by solid-state magic-angle-spinning NMR spectroscopy. *Nature* 420:98-102

Cavanagh, J., W.J. Fairbrother, A.G. Palmer, and N.J. Skelton. 1996. Protein NMR Spectroscopy. Academic Press, San Diego

Chattopadhyay, A., and K.G. Harikumar. 1996. Dependence of critical micelle concentration of a zwitterionic detergent on ionic strength: implications in receptor solubilization. *FEBS Lett.* 391:199-202

Chou, J.J., J.L. Baber, and A. Bax. 2004. Characterization of phospholipid mixed micelles by translational diffusion. *J. Biomol. NMR* 29:299-308

Chou, J.J., J.D. Kaufman, S.J. Stahl, P.T. Wingfield, and A. Bax. 2002. Micelle-induced curvature in a water-insoluble HIV-1 env peptide revealed by NMR dipolar coupling measurement in stretched polyacrylamide gel. *J. Am. Chem. Soc.* 124:2450-2451

Clore, G.M., A. Szabo, A. Bax, L.E. Kay, P.C. Driscoll, and A.M. Gronenborn. 1990. Deviations from the simple two-parameter model-free approach to the interpretation of nitrogen-15 nuclear magnetic relaxation of proteins. *J. Am. Chem. Soc.* 112:4989-4991

Czerski, L., and C.R. Sanders. 2000. Functionality of a membrane protein in bicelles. *Anal. Biochem.* 284:327-333

Damberg, P., J. Jarvet, P. Allard, U. Mets, R. Rigler, and A. Gräslund. 2002. ^{13}C-^{1}H NMR relaxation and fluorescence anisotropy decay study of tyrosine dynamics in motilin. *Biophys. J.* 83:2812-2825

Danielsson, J., J. Jarvet, P. Damberg, and A. Gräslund. 2002. Translational diffusion by PFG-NMR on full length and fragmets of the Alzheimer Aβ (1-40) peptide. Determination of hydrodynamic radii of random coil peptides of varying length. *Magnet. Reson. Chem.* 40:S89-S97

Deamer, D. 1997. The first living systems: a bioenergetic perspective. *Microbiol. Mol. Biol. Rev.* 61:239-261

Deisenhofer, J., and H. Michel. 1989. The photosynthetic reaction center from the purple bacterium *Rhodopseudomonas viridis*. *Science* 245:1463-1475

Derossi, D., A.H. Joliot, G. Chassaing, and A. Prochiantz. 1994. The third helix of the Antennapedia homeodomain translocates through biological membranes. *J. Biol. Chem.* 269:10444-10450

Dobson, C.M. 2003. Protein folding and misfolding. *Nature* 426:884-890

Drin, G., H. Déméné, J. Temsamani, and R. Brasseur. 2001. Translocation of the pAntp peptide and its amphipathic analogue AP-2AL. *Biochemistry* 40:1824-1834

Edmondson, S., N. Khan, J. Shriver, J. Zdunek, and A. Gräslund. 1991. The solution structure of motilin from NMR distance constraints, distance geometry, molecular dynamics, and an iterative full relaxation matrix refinement. *Biochemistry* 30:11271-11279

Ellena, J.E., M.C. Burnitz, and D.S. Cafiso. 2003. Location of the myristoylated alanine-rich c-kinase substrate (MARCKS) effector domain in negatively charged phsopholipid bicelles. *Biophys. J.* 85:2442-2448

Ellena, J.F., L.S. Lepore, and D.S. Cafiso. 1993. Estimating lipid lateral diffusion in phospholipid vesicles from ^{13}C spin-spin relaxation. *J. Phys. Chem.* 97:2952-2957

Ellena, J.F., J. Moulthrop, J. Wu, M. Rauch, S. Jaysinghne, J.D. Castle, and D.S. Cafiso. 2004. Membrane position of a basic aromatic peptide that sequesters phosphatidylinositol 4,5 bisphosphate determined by site-directed spin labeling and high-resolution NMR. *Biophys. J.* 87:3221-3233

Evans, D.F., and H. Wennerström. 1999. The Colloidal Domain. Where Physics, Chemistry, Biology and Technology meet. Wiley-VHC, New York

Faham, S., and J.U. Bowie. 2002. Bicelle crystallization: a new method for crystallizing membrane proteins yields a monomeric bacteriorhodopsin structure. *J. Mol. Biol.* 316:1-6

Fieghner, S.D., C.P. Tan, K.K. McKee, O.C. Palyha, D.L. Hreniuk, S.S. Pong, C.P. Austin, D. Figueroa, D. MacNeil, M.A. Cascieri, R. Nargund, M. Abramovitz, R. Stocco, S. Kargman, G. O'Neill, L.H. Van der Ploeg, J. Evans, A.A. Patchett, R.G. Smith, and A.D. Howard. 1999. Receptor for motilin identified in the human gastrointestinal system. *Science* 284:2184-2188

Flory, P.J. 1969. Statistical Physics of Chain Molecules. Wiley, New York

Frauenfelder, H., S.G. Sligar, and P.G. Wolynes. 1991. The energy landscapes and motions of proteins. *Science* 254:1598-1603

Funasaki, N., S. Hada, and S. Neya. 1991. Odd-even alternation in the aggregation number dependence of stepwise aggregation constants. *J. Phys. Chem.* 95:1846-1850

Gaemers, S., and A. Bax. 2001. Morphology of three lyotropic liquid crystalline biological NMR media studied by translational diffusion anisotropy. *J. Am. Chem. Soc.* 123:12343-11235

Gennis, R.B. 1989. Biomembranes: Molecular Structure and Function. Springer, New York

Glatti, A., X. Daura, D. Seebach, and W.F. van Gunsteren. 2002. Can one derive the conformational preference of a beta-peptide from its CD spectrum? *J. Am. Chem. Soc.* 124:12972-12978

Glover, K.J., J.A. Whiles, M.J. Wood, G. Melacini, E.A. Komives, and R.R. Vold. 2001a. Conformational dimorphism and transmembrane orientation of prion protein residues 110-136 in bicelles. *Biochemistry* 40:13137-13142

Glover, K.J., J.A. Whiles, G. Wu, N.-J. Yu, R. Deems, J.O. Struppe, R.E. Stark, E.A. Komives, and R.R. Vold. 2001b. Structural evaluation of phospholipid bicelles

for solution-state studies of membrane-associated biomolecules. *Biophys. J.* 81:2163-2171
Grell, E. 1981. Membrane Spectroscopy. Springer, New York
Halle, B. 1991. Theory of spin relaxation by diffusion on curved surfaces. *J. Am. Chem. Soc.* 94:3150-3168
Halle, B., and M. Davidovic. 2003. Biomolecular hydration: from water dynamics to hydrodynamics. *Proc. Natl. Acad. Sci. U. S. A.* 100:12135-12140
Halle, B., and H. Wennerström. 1981. Interpretation of magnetic resonance data from water nuclei in heterogeneous systems. *J. Chem. Phys.* 75:1928-1943
Hare, B.J., J.H. Prestegard, and D.M. Engelman. 1995. Small angle x-ray scattering studies of magnetically oriented lipid bilayers. *Biophys. J.* 69:1891-1896
Hauser, H. 2000. Short-chain phospholipids as detergents. *Biochim. Biophys. Acta* 1508:164-181
Hegde, R.S., J.A. Mastrianni, M.R. Scott, K.A. DeFea, P. Tremblay, M. Torchia, S.J. DeArmond, S.B. Prusiner, and V.R. Lingappa. 1998. A transmembrane form of the prion protein in neurodegenerative disease. *Science* 279:827-834
Hegde, R.S., P. Tremblay, D. Groth, S.J. DeArmond, S.B. Prusiner, and V.R. Lingappa. 1999. Transmissible and genetic prion diseases share a common pathway of neurodegeneration. *Nature* 402:822-826
Henry, G.D., and B.D. Sykes. 1994. Methods to study membane protein structure in solution. *Meth. Enzymol.* 239:515-535
Hinz, H.J., and J.M. Sturtevant. 1972. Calorimetric investigation of the influence of cholesterol on the transition properties of bilayers formed from synthetic L-lecithins in aqueous suspension. *J. Biol. Chem.* 247:3697-3700
Itoh, Z. 1997. Motilin and clinical applications. *Pept.* 18:593-608
Itri, R., and L.Q. Amaral. 1991. Distance distribution function of soduim dodecyl sulfate micelles by X-ray scattering. *J. Phys. Chem.* 95:423-427
Jarvet, J., P. Allard, A. Ehrenberg, and A. Gräslund. 1996. Spectral-Density Mapping of a $^{13}C^{\alpha}$-$^{1}H^{\alpha}$ Vector Dynamics Using Dipolar Relaxation Rates Measured at Several Magnetic Fields. *J. Magnet. Reson.* 111:23-30
Jarvet, J., J. Zdunek, P. Damberg, and A. Gräslund. 1997. Three-dimensional structure and position of porcine motilin in sodium dodecyl sulfate micelles determined by ^{1}H NMR. *Biochemistry* 36:8153-8163
Jeener, J., B.H. Meier, P. Bachmann, and R.R. Ernst. 1979. Investigation of exchange processes by two-dimensional NMR spectroscopy. *J. Chem. Phys.* 71:4546-4553
Kahn, N., A. Gräslund, A. Ehrenberg, and J. Shriver. 1990. Sequence-specific ^{1}H NMR assignments and secondary structure of porcine motilin. *Biochemistry* 29:5743-5751
Karplus, M. 1959. Contact electron-spin coupling of nuclear magnetic moments. *J. Chem. Phys.* 30:11-15
Killian, J.A. 2003. Synthetic peptides as models for intrinsic membrane proteins. *FEBS Lett.* 555:134-138
Lakowicz, J.R. 1999. Principles of Fluorescence Spectroscopy. Kluwer, New York
Lee, L.K., M. Rance, W.J. Chazin, and A.G.III. Palmer. 1997. Rotational anisotropy of proteins from simultaneous analysis of ^{15}N and $^{13}C^{\alpha}$ nuclear spin relaxation. *J. Biomol. NMR* 9:287-298
Lin, T.-L., C.-C. Liu, M.F. Roberts, and S.-H. Chen. 1991. Structure of mixed short chain lecithin/long-chain lecithin aggregates studied by small-angle neutron scattering. *J. Phys. Chem.* 95:6020-6027

Lin, T.S., S.H. Chen, N.E. Gabriel, and M.F. Roberts. 1986. Use of small-angle neutron scattering to determine the structure and interaction of dihexanoylphosphatidylcholine micelles. *J. Am. Chem. Soc.* 108:3499-3507

Lindberg, M., H. Biverståhl, A. Gräslund, and L. Mäler. 2003. Structure and positioning comparison of two variants of penetratin in two different membrane mimicking systems by NMR. *Eur. J. Biochem.* 270:3055-3063

Lindberg, M., and A. Gräslund. 2001. The position of the cell penetrating peptide penetratin in SDS micelles determined by NMR. *FEBS Lett.* 497:39-44

Lindberg, M., J. Jarvet, U. Langel, and A. Gräslund. 2001. Secondary structure and position of the cell-penetrating peptide transportan in SDS micelles as determined by NMR. *Biochemistry* 40:3141-3149

Lindman, B., N. Kamenka, M.C. Puyal, R. Rymdén, and P. Stilbs. 1984. Micelle formation of anionic and cationic surfactants from Fourier transform proton and lithium-7 nuclear magnetic resonance and tracer self-diffusion studies. *J. Phys. Chem.* 88:5048-5057

Lindorff-Larsen, K., R.B. Best, M.A. Depristo, C.M. Dobson, and M. Vendruscolo. 2005. Simultaneous determination of protein structure and dynamics. *Nature* 433:128-132

Lipari, G., and A. Szabo. 1982a. Model-free approach to the interpretation of nuclear magnetic resonance relaxation in macromolecules. 1. Theory and range of validity. *J. Am. Chem. Soc.* 104:4546-4559

Lipari, G., and A. Szabo. 1982b. Model-free approach to the interpretation of nuclear magnetic resonance relaxation in macromolecules. 2. Analysis of experimental results. *J. Am. Chem. Soc.* 104:4559-4570

Luchette, P.A., T.N. Vetman, R.S. Prosser, R.E.W. Hancock, M.P. Nieh, C.J. Glinka, S. Krueger, and J. Katsaras. 2001. Morphology of fast-tumbling bicelles: a small angle neutron scattering and NMR study. *Biochim. Biophys. Acta* 1513:83-94

Lundberg, M., and M. Johansson. 2002. Positively charged DNA-binding proteins cause apparent cell membrane translocation. *Biochem. Biophys. Res. Commun.* 291:376-371

Magzoub, M. 2004. Cell-Penetrating Peptides in Model Membrane Systems. Doctoral thesis. Stockholm University, Stockholm

Magzoub, M., L.E.G. Eriksson, and A. Gräslund. 2002. Conformational states of the cell-penetrating peptide penetratin when interacting with phospholipid vesicles: effects of surface charge and peptide concentration. *Biochim. Biophys. Acta* 1563:53-63

Magzoub, M., L.E.G. Eriksson, and A. Gräslund. 2003. Comparisom of the interaction, positioning, structure induction and membrane perturbation of cell-penetrating peptides and non-translocating variants with phospholipid vesicles. *Biophys. Chem.* 103:271-288

Magzoub, M., and A. Gräslund. 2004. Cell-penetrating peptides: from inception to application. *Q. Rev. Biophys.* 37:147-195

Magzoub, M., K. Kilk, L.E.G. Erikssom, U. Langel, and A. Gräslund. 2001. Interaction and structure induction of cell-penetrating peptides in the presence of phospholipid vesicles. *Biochim. Biophys. Acta* 1512:77-89

Mäler, L., J. Blankenship, M. Rance, and W.J. Chazin. 2000. Site-site communication in the EF-hand Ca2+-binding protein calbindin D9k. *Nat. Struct. Biol.* 7:245-250

Marcotte, I., and M. Auger. 2005. Bicelles as model membranes for solid- and solution-state NMR studies of membrane peptides and proteins. *Concepts Magnet. Reson.* 24:17-37

Marcotte, I., F. Separovic, M. Auger, and S.M. Gagné. 2004. A multidimensional ^{1}H NMR investigation of the conformation of methionine-enkephalin in fast tumbling bicelles. *Biophys. J.* 86:1587-1600

Matsuzaki, K. 1999. Why and how are peptide-lipid interactions utilized for self-defense? Magainins and tachyplesins as archetypes. *Biochim. Biophys. Acta* 1462:1-10

Mayer, C., G. Gröbner, K. Müller, K. Weisz, and G. Kothe. 1990. Orientation-dependent deuteron spin-lattice relaxation times in bilayer membranes: characterization of the overall lipid motion. *Chem. Phys. Lett.* 165:155-161

Mazer, N.A., G.B. Benedek, and M.C. Carey. 1980. Quasielastic light-scattering studies of aqueous biliary lipid systems. Mixed micelle formation in bile salt-lecithin solutions. *Biochemistry* 19:601-615

McConnell, H.M. 1958. Reaction rates by nuclear magnetic resonance. *J. Chem. Phys.* 28:430-431

Millet, O., D.R. Muhandrin, N.R. Skrynnikov, and L.E. Kay. 2002. Deutrium spin probes of side-chain dynamics in proteins. 1. Measurements of five relaxation rates per deuteron in ^{13}C-labeled and fractionally ^{2}H-enriched proteins in solution. *J. Am. Chem. Soc.* 124:6439-6448

Mills, R. 1973. Self-diffusion in normal and heavy water in the range of 1-45^{o}. *J. Phys. Chem.* 77:685-688

Nagle, J.F., and S. Tristram-Nagle. 2000. Structure of lipid bilayers. *Biochim. Biophys. Acta* 1469:159-195

Nieh, M.P., V.A. Raghunathan, C.J. Glinka, T.A. Harroun, G. Pabst, and J. Katsaras. 2004. Magnetically alignable phase of phospholipid "bicelle" mixtures is a chiral nematic made up of wormlike micelles. *Langmuir* 20:7893-7897

Orädd, G., and G. Lindblom. 2004. NMR Studies of lipid lateral diffusion in the DMPC/gramicidin D/water system: peptide aggregation and obstruction effects. *Biophys. J.* 87:980-987

Ott, C.M., and V.R. Lingappa. 2004. Signal sequences influence membrane integration of the prion protein. *Biochemistry* 43:11973-11982

Ottiger, M., and A. Bax. 1998. Characterization of magnetically oriented phospholipid micelles for measurement of dipolar couplings in macromolecules. *J. Biomol. NMR* 12:361-372

Pastor, R.W., R.M. Venable, M. Karplus, and A. Szabo. 1988. A simulation based model of NMR T_1 relaxation in lipid bilayer vesicles. *J. Chem. Phys.* 89:1128-1140

Pencer, J., G.F. White, and R.F. Hallett. 2001. Osmotically induced shape changes of large unilamellar vesicles measured by dynamic light scattering. *Biophys. J.* 81:2716-2728

Peng, J.W., and G. Wagner. 1992. Mapping of spectral density functions using heteronuclear NMR relaxation measurements. *J. Magnet. Reson.* 98:308-332

Perrin, F. 1934. Mouvement brownien d'un ellipsoïde. I. Dispersion diélectrique pour des molécules ellipsoïdales. *J. Phys. Radium.* 5:497-511

Perrin, F. 1936. Mouvement brownien d'un ellipsoïde. II Rotation libre er dépolarisation des fluorescences. Translation et diffusion de molécules ellipsoïdales. *J. Phys. Radium* 7:1-11

Persson, D., P.E. Thorén, E.K. Esbjörner, M. Goksör, P. Lincoln, and B. Nordén. 2004. Vesicle size-dependent translocation of penetratin analogs across lipid membranes. *Biochim. Biophys. Acta* 1665:142-155

Persson, D., P.E. Thorén, and B. Nordén. 2001. Penetratin-induced aggregation and subsequent dissociation of negatively charged phospholipid vesicles. *FEBS Lett.* 505:307-312

Pervushin, K., R. Riek, G. Wider, and K. Wüthrich. 1997. Attenuated T_2 relaxation by mutual cancellation of dipole-dipole couplings and chemical shift anisotropy inidcates an avenue to NMR structures of very large biological macromolecules in solution. *Proc. Natl. Acad. Sci. U. S. A.* 94:12366-12371

Prusiner, S.B. 1982. Novel proteinaceous infectious particles cause scrapie. *Science* 216:136-144

Prusiner, S.B. 1997. Prion diseases and the BSE crisis. *Science* 278:245-251

Ram, P., and J.H. Prestegard. 1988. Magnetic field induced ordering of bile salt/phospholipid micelles: new media for NMR structural investigations. *Biochim. Biophys. Acta* 940:289-294

Redfield, A.G. 1957. On the Theory of Relaxation Processes. *IBM J.* 1:19-31

Redfield, A.G. 1965. The theory of relaxation processes. *Adv. Magnet. Reson.* 1:1-32

Roosild, T.P., J. Greenwald, M. Vega, S. Castronovo, R. Riek, and S. Choe. 2005. NMR structure of Mistic, a membrane-integrating protein for membrane protein expression. *Science* 307:1317-1321

Sanders, C.R., A.K. Hoffmann, D.N. Gray, M.H. Keyes, and C.D. Ellis. 2004. French swimwear for membrane proteins. *Chem. Bio. Chem.* 5:423-426

Sanders, C.R., and J.H. Prestegard. 1990. Magnetically orientable phospholipid bilayers containing small amounts of a bile salt analogue, CHAPSO. *Biophys. J.* 58:447-460

Sanders, C.R., and J.P. Schwonek. 1992. Characterization of magnetically orientable bilayers in mixtures of dihexanoylphosphatidylcholine and dimyristoylphosphatidylcholine by solid-state NMR. *Biochemistry* 31:8898-8905

Sanders, C.R.I., and G.C. Landis. 1995. Reconstitution of membrane proteins into lipid-rich bilayered mixed micelles for NMR studies. *Biochemistry* 34:4030-4040

Sargent, D.F., and R. Schwyzer. 1986. Membrane lipid phaseas catalyst for peptide-receptor interactions. *Proc. Natl. Acad. Sci. U. S. A.* 83:5774-5778

Seelig, J. 1977. Deuterium magnetic resonance: theory and application to lipid membranes. *Q. Rev. Biophys.* 10:353-418

Simha, R. 1940. The influence of Brownian movement on the viscosity of solutions. *J. Phys. Chem.* 44:25-34

Singer, S.J., and G.L. Nicolson. 1972. Fluid mosaic model of the structure of cell membranes. *Science* 175:720-731

Skrynnikov, N.R., O. Millet, and L.E. Kay. 2002. Deutrium spin probes of side-chain dynamics in proteins. 2. Spectral density mapping and identification of nanosecond time-scale side-chain motions. *J. Am. Chem. Soc.* 124:6449-6460

Slichter, C.P. 1978. Principles of Magnetic Resonance. Springer, Heidelberg

Small, D.M. 1967. Physicochemical studies of cholesterol gallstone formation. *Gastroenterology* 52:607-610

Small, D.M., M.C. Bourgès, and D.G. Dervichian. 1966. The biophysics of lipidic associations. I. The ternary systems: lecithin-bile salt-water. *Biochim. Biophys. Acta* 125:563-580

Small, D.M., S.A. Penkett, and D. Chapman. 1969. Studies on simple and mixed bile salt micelles by nuclear magnetic resonance spectroscopy. *Biochim. Biophys. Acta* 176:178-189

Söderman, O., P. Stilbs, and W. Price. 2004. NMR studies of surfactants. *Concepts Magnet. Reson.* 23A:121-135

Stejskal, E.O., and J.E. Tanner. 1965. Spin diffusion measurements: spin echoes in the presence of a time-dependent field gradient. *J. Phys. Chem.* 42:288-292

Struppe, J., and R.R. Vold. 1998. Dilute bicellar solutions for structural NMR work. *J. Magn. Reson.* 135:541-546

Struppe, J., J.A. Whiles, and R.R. Vold. 2000. Acidic phospholipid bicelles: a versatile model membrane system. *Biophys. J.* 78:281-289

Terrone, D., S.L. Sang, L. Roudaia, and J.R. Silvius. 2003. Penetratin and related cell-penetrating cationic peptides can translocate across lipid bilayers in the presence of a transbilayer potential. *Biochemistry* 42:13787-13799

Thorén, P.E., D. Persson, E.K. Esbjörner, M. Goksör, P. Lincoln, and B. Nordén. 2004. Membrane binding and translocation of cell-penetrating peptides. *Biochemistry* 43:3471-3489

Thorén, P.E., D. Persson, M. Karlsson, and B. Nordén. 2000. The antennapedia peptide penetratin translocates across lipid bilayers - the first direct observation. *FEBS Lett.* 482:265-268

Tjandra, N., and A. Bax. 1997. Direct measurement of distances and angles in biomolecules by NMR in a dilute liquid crystalline medium. *Science* 278:111-1114

Tolman, J.R., J.M. Flanagan, M.A. Kennedy, and J.H. Prestegard. 1995. Nuclear magnetic dipole interactions in field-oriented proteins: information for structure determination in solution. *Proc. Natl. Acad. Sci. U. S. A.* 92:9279-9283

Torres, J., T.J. Stevens, and M. Samsó. 2003. Membrane proteins: the 'Wild West' of structural biology. *Trends Biochem. Sci.* 28:137-144

Triba, M.N., D.E. Warschawski, and P.F. Devaux. 2005. Reinvestigation by phosphorus NMR of lipid distribution in bicelles. *Biophys. J.* 88:1887-1901

van Dam, L., G. Karlsson, and K. Edwards. 2004. Direct observation and characterization of DMPC/DHPC aggregates under conditions relevant for biological solution NMR. *Biochim. Biophys. Acta* 1664:241-256

Vereb, G., J. Szöllosi, J. Matkó, P. Nagy, T. Farkas, L. Vigh, L. Mátyus, T.A. Waldmann, and S. Damjanovich. 2003. Dynamic, yet structured: The cell membrane three decades after the Singer-Nicolson model. *Proc. Natl. Acad. Sci. U. S. A.* 100:8053-8058

Vold, R.R., and R.S. Prosser. 1996. Magnetically oriented phospholipid bilayer micelles for structural studies of polypeptides. Does the ideal bicelle exist? *J. Magnet. Reson.* 113:267-271

Vold, R.R., S.R. Prosser, and A.J. Deese. 1997. Isotropic solutions of phospholipid bicelles: a new membrane mimetic for high-resolution NMR studies of polypeptides. *J. Biomol. NMR* 9:329-335

Wang, J., J.R. Schnell, and J.J. Chou. 2004. Amantadine partition and localization in phospholipid membrane: a solution NMR study. *Biochem. Biophys. Res. Commun.* 324:212-217

Wangsness, R.K., and F. Bloch. 1953. The dynamical theory of nuclear induction. *Phys. Rev.* 89:728-739

Wennerström, H., G. Lindblom, and B. Lindman. 1974. Theoretical aspects on the NMR of quadrupolar ionic nuclei in micellar solutions and amphiphilic liquid crystals. *Chem. Scr.* 6:97-103

Whiles, J.A., R. Brasseur, K.J. Glover, G. Melacini, E.A. Komives, and R.R. Vold. 2001. Orientation and effects of mastoparan X on phospholipid bicelles. *Biophys. J.* 80:280-293

Whiles, J.A., R. Deems, R.R. Vold, and E.A. Dennis. 2002a. Bicelles in structure-function studies of membrane-associated proteins. *Bio Org. Chem.* 30:431-442

Whiles, J.A., K.J. Glover, R.R. Vold, and E.A. Komives. 2002b. Methods for studying transmembrane peptides in bicelles: consequences of hydrophobic mismatch and peptide sequence. *J. Magnet. Reson.* 158:149-156

Wilkins, D.K., S.B. Grimshaw, V. Receveur, C.M. Dobson, J.A. Jones, and L.J. Smith. 1999. Hydrodynamic radii of native and denatured proteins measured by pulse field gradient NMR techniques. *Biochemistry* 38:16424-16431

Wimley, W.C., and T.E. Thompson. 1990. Exchange and flip-flop of dimyristoylphosphatidylcholine in liquid-crystalline, gel, and two-component, two-phase large unilamellar vesicles. *Biochemistry* 29:1296-1303

Wishart, D.S., and B.D. Sykes. 1994. Chemical shifts as a tool for structure determination. *Meth. Enzymol.* 239:363-392

Woese, C. 2004. A new biology for a new century. *Microbiol. Mol. Biol. Rev.* 68:173-186

Woessner, D.E. 1962. Nuclear spin relaxation in ellipsoids undergoing rotational brownian motion. *J. Chem. Phys.* 37:647-654

Wüthrich, K. 1986. NMR of Proteins and Nucleic Acids. Wiley-Interscience, New York

Yeagle, P.L. 2005. The Structure of Biological Membranes. CRC press, Boca Raton

ACKNOWLEDGEMENTS

Efter fem års forskarstuderande vid avdelningen för biofysik är listan lång på personer som både genom sina kunskaper och sina personligheter gjort denna tid till både intressant och rolig. Jag vill tacka:

min handledare, **Lena Mäler**, för att du på ett mycket bra sätt balanserat mellan att ge mig frihet men också stabilitet och kontinuitet i min forskning.

Astrid Gräslund, det är till stor del din förtjänst att biofysik är en mycket bra arbetsplats.

the co-authors of the papers: **Franz Hagn**, **Jonas Almqvist**, Elsa **Bárány-Wallje**, **Henrik Biverståhl**, **Astrid Gräslund** and **Lena Mäler** for good collaborations

alla ni som gett synpunkter på denna av handling: **Lena Mäler**, **Astrid Gräslund**, **Göran Eriksson**, **Åke Wieslander**, **Peter Damberg**, **Joe DePierre** och **Stefan Nordlund**

mina rumskamrater, **Jens Danielsson** och **Henrik Biverståhl**, för stenhårda dominodueller, fredagshissmusik, samt andra bidrag till en trevlig stämning

the physicalists **Vasco Castro** and **Jonas Danielsson**, for Friday beer and for glorious badminton and football tournaments

Haidi Astlind, som med en ängels tålamod håller ordning på allehanda kvitton och papper som tenderar att försvinna

Torbjörn Astlind, alla spektroskopisters och datoranvändares helgon

Britt-Marie Olsson, för en schysst labmiljö

All past and present people at the biophysics division

Min mor och min far för kärlek och uppmuntran

Julia, min sötnos, jag är så glad att jag träffat Dig!

Part 3: Results